5-2018

Combinational Therapy to Mitigate α-Dicarbonyl Toxicity

Jessica Ramirez
Dominican University of California

https://doi.org/10.33015/dominican.edu/2018.bio.03

Combinational Therapy to Mitigate α-Dicarbonyl Toxicity

By

Jessica Lisette Ramirez

A culminating thesis submitted to the faculty of Dominican University of California in partial fulfillment of the requirements for the degree of Master of Science in Biology

San Rafael, California

May, 2018

This thesis, written under the direction of candidate's thesis advisor and approved by the thesis committee and the MS Biology program director, has been presented and accepted by the Department of Natural Sciences and Mathematics in partial fulfillment of the requirements for the degree of Master of Science in Biology at Dominican University of California. The written content presented in this work represents the work of the candidate alone.

Jessica Ramirez	05 /11/2018
Candidate	
Pankaj Kapahi	05 /11/2018
Thesis Advisor	
Kiowa Bower	05 /11/2018
Second Reader	
Meredith Protas	05/11/2018
Program Director	

Table of contents

List of Figures

Abstract

Diabetes mellitus is a metabolic disease characterized by hyperglycemia that affects 30 million children and adults in the United States alone. Patients suffering from diabetes have high concentrations of reactive α-dicarbonyls (α-DCs) like, methylglyoxal (MGO). The abundance of α-DCs form advanced glycation end products (AGEs); in turn, the accumulation of AGEs has been linked to secondary complications. Secondary complications include diabetic neuropathy, nephropathy and cardiomyopathy. A recently discovered TRPA-1-Nrf-2 pathway is a conserved mechanism in vertebrates and invertebrates that detoxifies α-DCs; however, regulators that activate the detoxification mechanism are currently unknown. Several supplement grade compounds were screened for TRPA-1-Nrf2 induced activity in *Caenorhabditis elegans*. The drug screen revealed several candidates that decreased methylglyoxal levels using the TRPA-1-Nrf-2 pathway. Regulatory mechanisms that trigger this detoxification pathway open up avenues for therapeutic studies. Candidates were utilized to determine their therapeutic efficacy in mammalian *in vitro* studies, in the background of methylglyoxal stress. In this work, we pursue combinational therapy to identify a more effective approach at mitigating neurotoxicity. We show that a five-compound combination ameliorates methylglyoxal stress in multiple dopaminergic cell lines: N27, PC12 and SH-SY5Y. Results indicate that combinational therapy counteracts methylglyoxal stress more effectively than compounds used in isolation. Data suggests that the five-compound mixture can be used as a potential supplement to treat diabetic complications in patients suffering from long term diabetes.

Specific Aims

1. *Validate individual candidates from drug screen in mammalian cell culture.*

We will expose dopaminergic cells to an α-dicarbonyl (methylglyoxal) in order to cause neuronal damage; cells will exhibit neurite retraction. 6 different concentrations: (1 nM, 10 nM, 100 nM, 1μM, 10 μM, 100 μM) of each individual compound, from the drug screen, will be tested. At 5 different time points (0 hr, 3 hr, 6 hr, 12 hr, and 24 hr) photos will be taken. We will measure the neurite length, using Image J software, to determine if the compounds prevent the cells neurite from retracting. We hypothesize that the compounds will rescue cells from methylglyoxal-induced neuronal damage, essentially preserving the cells neurite length. Once all the compounds are tested, we will identify eight compounds that rescue neuronal damage. We will focus on one specific time point that works best.

2. *Test various compound combinations to identify a more effective approach in ameliorating methylglyoxal stress.*

Our hypothesis is that a combination of compounds will serve as a better therapeutic for ameliorating methylglyoxal stress. Using the N27 cell line, 6 different concentrations of double, triple, and quadruple and quintuple combinations will be tested at 24 hours and the neurite length will be quantified. We will determine if the combination alleviates methylglyoxal-induced neurotoxicity better than the individual compounds.

3. *Test the best combination in various cell lines to confirm its therapeutic efficacy.*

Once we identify the two best combinations using the N27 cell line, we will test the combination in two additional cell lines: PC12 and SH-SY5Y. This will confirm that the

combination protects cells against methylglyoxal neuronal damage. We will test each combination at 6 different concentrations: 1 nM, 10 nM, 100 nM, 1 µM, 10 µM, 100 µM. We will measure the neurite length, using Image J software to determine if the compounds are able to prevent retraction of the neurite.

4. *Test the best compound combination in various cell lines to investigate its neuroprotective capacity against MPP^+-induced cellular damage.*

We will test the two best combinations in N27, PC12 and SH-SY5Y cell lines to study its neuroprotective capacity against a neurotoxin, MPP^+. We will test each combination at 6 different concentrations: 1 nM, 10 nM, 100 nM, 1 µM, 10 µM, 100 µM. We will measure the neurite length, using Image J software to determine if the compounds are able to prevent retraction of the neurite.

Introduction

Aging is a major risk factor for a number of diseases including diabetes. Diabetes mellitus (DM) is a metabolic disorder characterized by high blood glucose levels. This can be a result of environmental or genetic factors. Metabolism of fat, protein and carbohydrates are affected by DM, resulting in deficiencies in insulin secretion in type 1 diabetes (1). Type 2 diabetes arises from multiple factors, including; insulin resistance, obesity, and hyperglycemia. While patients with type 2 diabetes can control their glycemic levels, the disease still progresses. This indicates that there is an underlying mechanism responsible for DM progression independent of insulin and glucose (2). Due to the amount of people who are diagnosed with DM, there is rising concern about a global diabetes epidemic (3). In 2014, 366 million adults and children were reported to have diabetes worldwide (4). Diabetes mellitus has long-term effects including injury, and failure or dysfunction of several organs. Long-term diabetes increases the risk of developing multiple secondary complications including: nephropathy resulting in renal failure, retinopathy resulting in vision loss, peripheral neuropathy resulting in nerve pain, foot amputation, ulcers, and cardiomyopathy resulting in cardiovascular dysfunctions (5). The molecular cause of type 2 diabetes and secondary pathologies are not fully understood, here we focus on the underlying mechanism.

By studying the mechanisms that dictate the onset of diabetes, we open avenues to identify novel methods that may be used to counter secondary pathologies. Chronic hyperglycemia, lipid peroxidation, and anaerobic glycolysis form unavoidable byproducts, called α-dicarbonyls (α-DC) **(Figure 1)** (6). Increased levels of α-dicarbonyls like methylglyoxal (MGO), glyoxal (GO) and 3-deoxyglucasone (3-DG), have been

found in the blood plasma of patients with diabetes (7). α-dicarbonyls are toxic metabolites and potent glycation agents that bind with DNA, lipids, and proteins causing irreversible damage, ultimately altering the function and structure of these macromolecules (8). In this thesis, MGO is a α-dicarbonyl we primarily focus on to study its influence on diabetic pathologies. Methylglyoxal is an environmental and/or bacterial toxin that is spontaneously formed from triosephosphates with anaerobic glycolysis (9). The increased production of MGO and the impaired function in detoxifying this toxic, reactive metabolite could cause type 2 diabetes, and therefore be the reason why we observe phenotypes in diabetic patients including: obesity, insulin resistance and hyperglycemia (2).

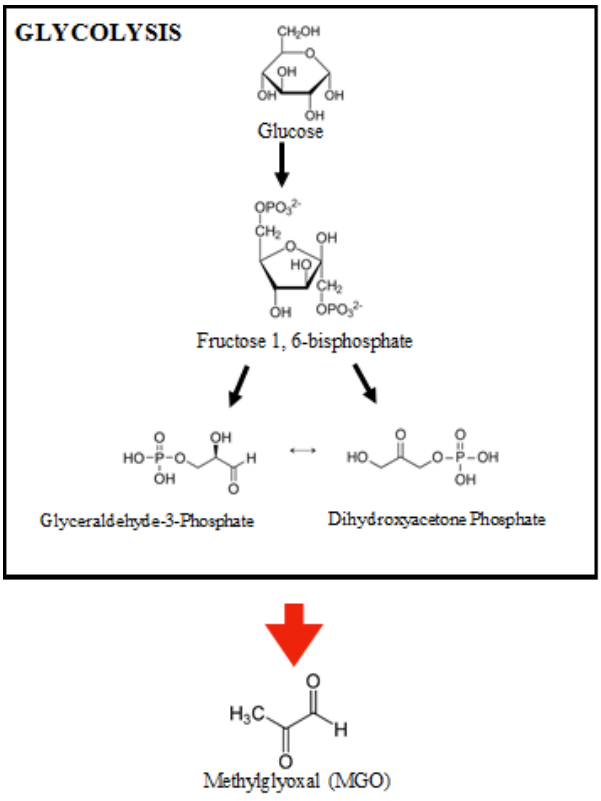

Figure 1: **Formation of α-dicarbonyls (e.g. methylglyoxal/MGO)**.
Methylglyoxal is an unavoidable byproduct of glycolysis. Fragmentations of glycolytic intermediates glyceraldehyde-3-phosphate and dihydroxyacetone phosphate produce α-dicarbonyls such as, methylglyoxal.

Hyperglycemia generates the endogenous metabolite, MGO, which is responsible for the glycation of proteins (10). Glycation is a process that occurs non-enzymatically. MGO interacts with arginine and lysine residues of macromolecules, forming advanced glycation end products (AGEs) **(Figure 2)** (11). High levels of exogenous MGO administration have been studied in both *in vivo* and *in vitro* models, resulting in hypercholesterolemia, insulin resistance, accumulation of collagen in kidneys, and microvascular degeneration (12–14). MGO has shown to directly increase the amount of reactive oxidative species, resulting in cell death (15). Oxidative stress and AGE accumulation induces hyperglycemia, playing a contributing role to the development of diabetes (16).

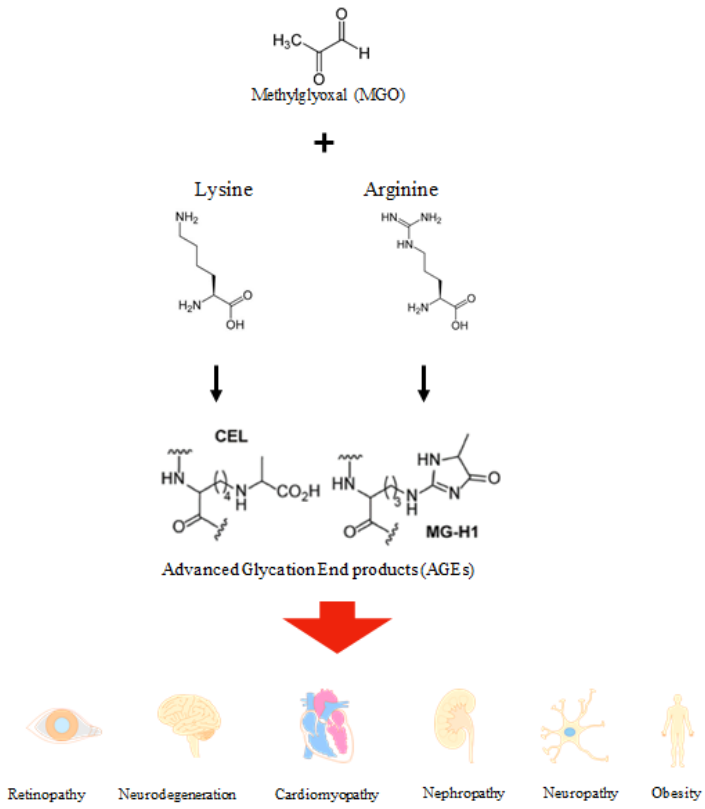

Figure 2: **Methylglyoxal-derived advanced glycation end-products (AGEs) mediate age-associated pathologies.**
This figure illustrates the formation of methylglyoxal-derived AGEs: Nε-carboxyethyl-lysine/CEL and methylglyoxal-hydroimidazolone/MG-H1. The accumulation of AGEs in various tissues results in a variety of disease.

The accumulation of AGEs, such as Nε-carboxyethyl-lysine (CEL) and methylglyoxal hydroimidazolone (MG-H1), is a causal risk factor for the rate of aging, ultimately modulating lifespan. Not only are AGEs generated endogenously, they are found in dietary sources as well. AGEs are abundant in animal-based foods that are rich in fat and protein when cooked at dry and high temperatures (17). AGEs crosslink proteins, causing an alteration in the protein's structure and function, and resulting in a diverse range of post translational modifications (17,18). AGEs not only derive from hyperglycemia, but are also generated as a result of increased oxidative stress even in the absence of high glucose levels. AGEs derived from dietary sources has been shown to exacerbate diabetic complications, causing accumulation of pro-inflammatory factors (19). AGEs are enzymatically broken down by the human body and eliminated through the kidneys (17). Accumulation of AGEs is abundant in serum and tissues, driving the development of diabetes complications and neurodegenerative disorders (20,21) **(Figure 2)**. AGEs tend to build up in the central nervous system, targeting areas with marked pathologies like the substantia nigra during Parkinson's disease (17).

α-Dicarbonyls are precursors of AGEs, forming three structural isomers that are ligands for the receptor of AGEs, referred to as RAGEs (22). AGE-associated pathologies are largely due to the activation of RAGEs (23). AGEs exert their effects upon binding to their receptor, RAGEs then induce intracellular signaling, inflammatory cytokines, and free radicals (10). This cascade stimulates inflammation and tissue injury, influencing the pathogenies of diabetes and neurodegenerative disorders (24,25).

Diabetic neuropathy

Approximately 30-50 percent of diabetic patients develop neuropathy as a secondary complication, making it one of the most common diabetic complications. Diabetic peripheral neuropathy occurs with aging, long term diabetes, lack of glycemic control, high blood pressure and elevated levels of lipid (26). Current studies are looking to prevent diabetic neuropathy by controlling glycemic levels (27). Roughly 16 percent of diabetic patients experience neuropathic pain (28). Hyperglycemia-induced oxidative stress promotes apoptosis of nerves, which leads to the pathogenesis of diabetic neuropathy (29). The accumulation of AGEs and their contributing role to oxidative stress have shown to be a mechanism involved in the pathogenesis of diabetic neuropathy (30). Increased oxidative stress results in impaired neural function, causing apoptosis of neurons, Schwann cells and glial cells located in the peripheral nervous system (31). Glycation of molecules present in the extracellular matrix impairs regeneration of neurons, inhibiting them from reproducing and influencing further damage (32). Loss of large and small nerve fibers can drive early signs of peripheral neuropathy, including: loss of vibratory sensation, altered proprioception, impairment of pain and sensitivity to touch. Patients who suffer from diabetic peripheral neuropathy develop symptoms such as sensory loss, numbness and stabbing/shooting sensation. Furthermore, sensory loss increases patient's risk for foot injury such as foot/leg infections and ulcers, which may lead to amputation of limbs. Diabetic peripheral neuropathy begins in the toes and works its way up the body, affecting the upper limbs (31). Symptoms such as altered proprioception cause imbalance and increase the risk of falling (33). The development of

these painful neuropathy symptoms hinders patients from performing normal daily activities and decreases quality of life.

Parkinson's disease (PD)

We study the link between diabetes and Parkinson's disease by recapitulating methylglyoxal-induced pathologies *in vitro*. Several epidemiological studies have linked hyperglycemia as a risk factor for Parkinson's Diseases (34). Parkinson's disease is a chronic neurodegenerative disorder characterized by the loss of dopaminergic neurons in the substantia nigra, located in the midbrain region (35). Depleted levels of dopaminergic activity in the striatum disable the coordination of movement, a major hallmark observed in Parkinson's patients (36). The neurodegeneration found in Parkinson's results from mitochondrial dysfunction and oxidative stress (36). Patients who suffer from Parkinson's disease develop symptoms such as bradykinesia, rigidity, resting tremor, and postural instability (37). Also, the development of PD can be largely due to the increased amounts of AGEs and receptor for AGEs (RAGEs) that have been found in the frontal cortex of patients. AGE production induces inflammation as a downstream effect, making it a key mechanism contributing to disease pathology. Damage caused by AGEs and the accumulation of aggregates results in cellular stress and neuronal death, in addition to a decline in proteostasis (38). Notably, the buildup of AGEs and its influence on neurodegeneration has led us to focus on the glyoxalase system as a potential therapeutic target to mediate AGEs formation and hinder AGEs-associated pathologies.

Studies have shown that therapies that benefit diabetic patients also show healing effects in PD patients (39). 1-Methy-4-phenyl-1,2,3,6-tetrahydropyridine (MPTP) toxicity has become a popular model for studying Parkinson's disease (40). In mice,

MPTP damages dopaminergic neurons in the substantia nigra and induces Parkinson's like symptoms (41). When MPTP oxidizes to 1-methyl-4-phenylpyridinium (MPP^+), the product is toxic. When MPP^+ is taken up by dopaminergic cells, MPP^+ interferes with mitochondrial respiration; hindering ATP formation and inducing oxidative stress. MPP^+ also disrupts calcium homeostasis, causing cellular damage (40).

MPTP is often used as a neurotoxin to induce a Parkinson's disease phenotype in animal models. Upon injection of MPTP, the mitochondrial complex I activity is inhibited and striatal dopaminergic neurons undergo cell death (41). Deletion of RAGE attenuated MPTP-related cell toxicity, reduced the pro-inflammatory effects caused by RAGE, and ultimately hindered the progression of PD (24).

α-Dicarbonyls detoxification

In this thesis, we focus on the underlying cause of the diabetes and neurodegenerative disorders. It is important to prevent toxic metabolites such as, reactive α-dicarbonyls, by enhancing a conserved detoxification mechanism. The abundance of α-dicarbonyls overwhelms the glyoxalase system and hinders the detoxification process (9). It is important to understand the mechanism that regulates stress response when α-dicarbonyls are present, as their detoxification is critical for limiting AGE formation. Previous research identified a conserved TRPA-1-Nrf2 signaling pathway, essential for the detoxification of α-dicarbonyls **(Figure 3)** (6). Upon activation of TRPA-1, the SKN-1/NRF-2 transcription factors upregulate the evolutionary conserved group of glyoxalases: glutathione-dependent (GLO1 and GLO2) and glutathione-independent (DJ1). These enzymes are responsible for catalyzing the detoxifying reaction by converting α-dicarbonyls to a much less toxic and less reactive metabolite, known as, D-

lactate **(Figure 4)** (3). MGO can be detoxified via the glyoxalase system (GLO1 and GLO2), dependent on the amount of reduced glutathione. However, under oxidative stress conditions the amount of reduced glutathione decreases, ultimately having a negative effect on the detoxification of MGO (42).

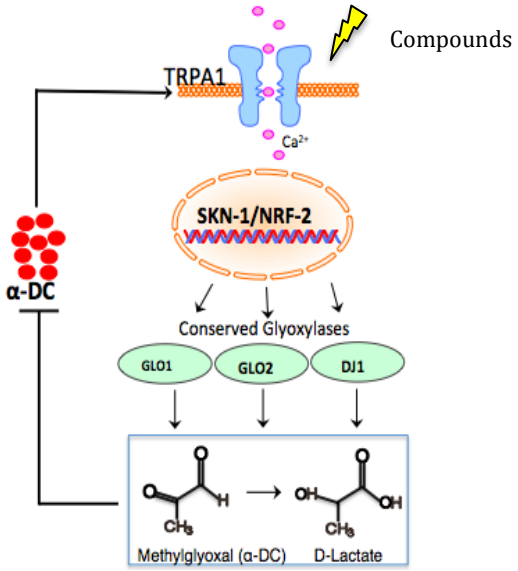

Figure 3: **Overview of TRPA-1-Nrf-2 detoxification mechanism.**
TRPA-1 receptor senses α-dicarbonyls (α-DC), causing a calcium influx, which activates SKN-1/Nrf-2 transcription factors, upregulating the conserved glyoxalases: GLO1, GlO2 and DJ1. The glyoxalases catalyze the reaction that detoxifies reactive α-DC (e.g. methylglyoxal) to D-Lactate.

Studies in mice have shown that impairment in GLO1 function result in hyperalgesia and nephropathy, which are symptoms found in patients suffering from diabetes (43,44). Furthermore, GLO1 impairment has also been shown to cause coronary artery disease and hypertension, evidence that a compromised detoxification mechanism induces secondary diabetic pathologies (45,46).

Glutathione-independent glyoxalase, DJ1, plays a critical role in the detoxification of α-dicarbonyls and is a genetic cause of early initiation of Parkinson's

disease (47). DJ1 is known for exhibiting neuroprotective properties against oxidative stress by reducing levels of reactive oxygen species and inhibiting cell death. DJ1 is also responsible for regulating dopamine synthesis. In addition to oxidative stress, with aging, DJ1 activity becomes impaired and has been associated with the pathogenesis of PD (36). Findings that DJ1 is involved in neurodegenerative disease allow researchers to study its neuroprotective role as a method for detoxifying α-dicarbonyls and preventing formation of AGEs.

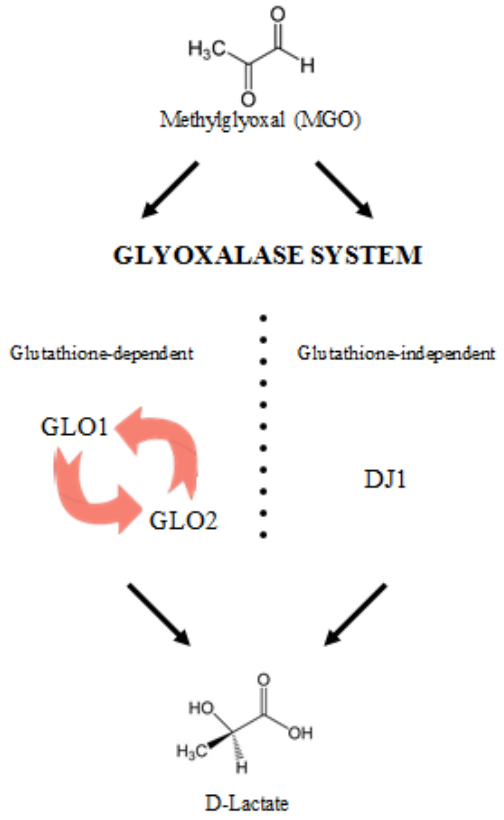

Figure 4: **Glyoxalase system detoxifies methylglyoxal.**
Methylglyoxal is detoxified to a less reactive product known as, D-lactate via glyoxalase system. Methylglyoxal detoxification occurs both independently and dependently on glutathione. Glutathione-dependent glyoxalase pathway is mediated by enzymes: glyoxalase 1 (GLO1) and glyoxalase 2 (GLO2). Glutathione-independent glyoxalase pathway is mediated by DJ1.

Previous research showed that exogenous administration of MGO caused *C. elegans* to develop hyperesthesia; a phenotype that mimicked diabetic complications. This further suggests that high levels of MGO are implicated in the progression of secondary pathologies (6). A high-throughput drug screen was performed to mitigate methylglyoxal toxicity in *C.elegans,* which revealed several candidate 'supplement-grade' compounds that are essentially safe for human consumption (6). Metabolomics analysis indicated that the compounds decreased levels of MGO and reversed the phenotype. They later determined their mechanism of action and concluded that the compounds lowered methylglyoxal levels via the TRPA-1-Nrf-2 pathway. Now that we understand the importance of glyoxalases in the detoxification of MGO, we can explore new avenues to study regulators of the glyoxalases as a potential treatment for MGO-mediated pathologies. Here, we validated the therapeutic efficacy of compounds found in the previous drug screen and further investigated their role on the detoxification of α-dicarbonyls in mammalian *in vitro* studies.

Combinational therapy

Due to the fact that diabetes is a progressive disorder, the use of single agents for treatment has been inadequate at controlling glycemic levels (48). Combinational therapy involving two or more agents is required for patients with type 2 diabetes to achieve lower glycemic levels (49).

Studies have shown that some compounds, when taken in combination improved glycemic control, lipid profiles, and prevented weight gain. They also showed that the combination worked to lower total cholesterol and free fatty acids (50). Combinational

therapy has been used in diabetic rats to halt the progression of diabetic neuropathy (51). In addition, the combination significantly reduced blood glucose levels and renal injury. This study also investigated the role that this combination had in decreasing oxidative stress and inhibiting inflammation. They discovered that the combination was a useful tool in reducing lipid peroxidation and inhibiting inflammatory cascade in diabetic rats.

Researchers have used a combination of natural compounds to investigate their therapeutic effects against MPTP-induced neurotoxicity (41). They saw that one of the compounds when used alone showed positive effects, but when used in combination, led to dramatic improvement in motor dysfunction, restoration of striatal neurotransmitter signaling, and reversal of depleted levels of nigrostriatal dopamine.

A combination of two compounds that induces GLO1 activity was used in a clinical trial on overweight and obese patients (52). The compounds administered individually were ineffective, but a combination of the two compounds improved insulin sensitivity in obese patients, increased clearance of methylglyoxal in the plasma of overweight patients and promoted weight loss and vascular health.

We are asking whether these supplement-grade compounds also work to mitigate α-dicarbonyl stress in humans/patients suffering from neuropathy as a result of long-term diabetes, and aging-associated neurodegenerative disorders such as Parkinson's disease.

Targeting MGO detoxification and prevention of AGE formation as a therapeutic approach

The increased production of glycating agents such as MGO is one of the main pathogenic mechanisms that lead to secondary complications associated with diabetes. Since MGO is still being produced, independent of blood glucose levels, a potential approach to attenuate its damaging effects is to inhibit the glycation reaction using "scavengers" (53). Scavengers are capable of interacting with MGO, essentially interfering with the glycation action and trapping it. This approach ultimately prevents the formation of AGEs and therefore impedes the development of secondary complications (54). The use of scavengers has shown to be beneficial in reducing levels of AGEs in various tissues and improving function of peripheral nerves in diabetic animals. Administration of these compounds to Type 2 diabetic patients have shown that they are effective at reducing MGO levels in blood plasma. Moreover, compounds that act as scavengers also have the ability to alleviate oxidative stress and increase the production of glutathione, which is essential for the detoxification of MGO via the glyoxalase system.

When exogenous MGO is administered to rats, scavenger compounds have been used as a treatment to decrease levels of AGES in adipose tissue (55). Both, *in vivo* and *in vitro* studies have shown that these compounds inhibit the formation of AGEs by scavenging α-dicarbonyl intermediates (56–58). They also have been shown to improve peripheral nerve function in diabetic rats by reducing AGE levels in tissue (59). Thus, these compounds are preventing AGE formation by directly reducing MGO levels with the aid of MGO scavenging and/or inducing activity of the glyoxalases.

AGE accumulation contributes to the pathogenesis of diabetic complications, leading to the development of therapies that hinder AGE formation. Combinational therapy has been used to decrease the levels of AGEs in the serum of diabetic mice, while monotherapy was not effective at all (60).

In this thesis, we determined the effects that single and combinational supplementation had on the MGO detoxification to prevent formation of AGEs. We used three different dopaminergic neuronal cell lines: N27, PC12 and SH-SY5Y. N27 is a cell line derived from the mesencephalic tissue of the rat and is used as a dopaminergic neuron model for *in vitro* studies (61). PC12, a rat cell line derived from the adrenal phaeochromocytoma, is used to study neurodegeneration (62). Finally, SH-SY5Y is a human cell line derived from a neuroblast from neural tissue, this cell line has become a popular cell model for PD research (63).

Our central focus is making these supplement-grade compounds relevant to human health by creating a supplement that can be readily available to patients. Oxidative stress is associated with both diabetes and Parkinson's disease, suggesting antioxidant properties within our supplement may prevent its detrimental effects. Antioxidant therapy can restore glutathione levels, enhancing the glyoxalase system and increasing the detoxification of MGO. We also seek to utilize compounds that possess neuroprotective properties. The combination we intend to create includes classes of compounds that have the same mechanism of action, the TRPA-1-Nrf-2 pathway which is responsible for regulating methylglyoxal detoxification.

The individual compounds have been previously used in various studies as supplements and have been shown to benefit diabetes and/or age-associated diseases. In this study we test several combinations to counteract methylglyoxal-induced and MPP^+-induced cellular damage in: N27, PC12 and SH-SY5Y cell lines. We have identified combinations that are more effective than the respective compounds administered individually. We chose a five drug mixture made up of L+N+T+Pi+Py. This compound mixture can be used to mitigate methylglyoxal-induced and MPP^+-induced neurotoxicity *in vitro,* and was shown to be more effective than the individual compounds tested. This study has given us the ability to further investigate the therapeutic effects of compound mixtures by administering them as a supplement to a diabetic mouse model. We believe that combinational therapy can mitigate α-dicarbonyl levels and prevent the onset of neurodegenerative disorders and diabetic complications such as neuropathy, cardiomyopathy, and nephropathy.

Material and Methods

Growth and differentiation of N27 cell line:

N27 dopaminergic cells were grown in Corning® RPMI 1640 L-media containing L-glutamine (Mediatech, Inc. Manassas, VA, USA) and 10% Fetal Bovine Serum (FBS; Gibco; Thermo Fisher Scientific, Inc., Waltham, MA, USA). Cells were incubated at 37˚C in a humidified air atmosphere containing 5% CO_2.

Neurite elongation was induced by addition of 1 mM of dibutyryl-cAMP (Enzo Life Sciences, Inc. Farmingdale, NY, USA) into the cell culture media. 48-72 hours following dibutyryl-cAMP treatment, cells exhibited extended neurites.

Growth and differentiation SH-SY5Y cell line:

The SH-SY5Y cells were grown in Dulbecco's modified Eagle's medium (DMEM; Hyclone; GE Healthcare Life Sciences, Logan UT, USA) and 10% heat-inactivated fetal bovine serum (FBS; Gibco; Thermo Fisher Scientific, Inc., Waltham, MA, USA). Cells were incubated at 37˚C in a humidified air atmosphere containing 5% CO_2.

Differentiation and neurite elongation was induced by addition of 10 µM of Retinoic Acid (Sigma-Aldrich, St. Louis, MO, USA) into the cell culture medium for 72 hours. 80 nM of 12-O-Tetradedanoylphorbol 13-acetate (Sigma-Aldrich, St. Louis, MO, USA) was administrated to the cell culture medium for an additional 72 hours.

Growth and differentiation PC12 cell line:

PC12 cells were grown in Dulbecco's Modification of Eagles Medium 4.5 g/L glucose, L-glutamine, sodium pyruvate (DMEM, 1X; Mediatech, Inc. Manassas, VA, USA), 10% HI inactivated Horse Serum (Gibco; Thermo Fisher Scientific, Inc.,

Waltham, MA, USA) and 5% heat-inactivated fetal bovine serum (FBS; Gibco; Thermo Fisher Scientific, Inc., Waltham, MA, USA). Cells were incubated at 37˚C in a humidified air atmosphere containing 5% CO2.

Differentiation and neurite elongation as induced by the addition of 50 ng/mL Corning® 7S Nerve Growth Factor, Mouse Natural (NGF; Discovery Labware, Inc. Bedford, MA, USA) to the cell culture media for 48-72 hours.

Neurite Length Imaging and Quantification

Cells were analyzed at 0, 3, 6, 12 and 24 hour after treatment with compounds. Cells were imaged with a Nikon Ti-Eclipse Perfect Focus System inverted microscope, equipped with a Cascase 512B camera (Photometrics, Tuscon, AZ). Quantification of neurite outgrowth of 75-100 randomly selected cells was done by manually measuring the length of a projection from the edge of the cell body (see Figure 4). One neurite of one individual cell will be quantified using Image J software (http://imagej.nih.gov/ij/).

Compound Administration under Methylglyoxal-Induced stress

Methylglyoxal (Sigma-Aldrich Corporation, St. Louis, MO, USA) was added at a concentration of 125 µM and individual drugs were administered in a dose dependent manner at increasing 10 fold increments starting from 1nM to 100 µM for 24 hours post differentiation. Ethanol and water was used as a vehicle control. Cells were imaged and quantified using the method found in the above section on titled "Neurite Length Imaging and Quantification".

Combination Administration under Methylglyoxal-Induced Stress

Methylglyoxal (Sigma-Aldrich Corporation, St. Louis, MO, USA) was added at a concentration of 125 µM in PC12 and N27 cell lines and 250 µM for the SH-SY5Y cell line. The combinations were administered for 24 hours post differentiation. The combinations were tested at 6 different concentrations: 1 nM, 10 nM, 100 nM, 1 µM, 10 µM and 100 µM. The two-compound combinations were comprised of equal amounts of two different compounds, essentially a 1:1 ratio mixture at all the above total concentrations as well. The three-compound mixture was comprised of an equal amount of each of the different compounds making up a 1:1:1 ratio. The four-compound mixture was made up of equal amounts of four different compounds. The five-compound mixture included a 1:1:1:1:1 ratio of five different compounds. When altering the volume of the each of compounds found in the five-compound combination, the mixture comprised of a 3:0.5:0.5:0.5:0.5 ratio.

Combination Administration under MPP^+ induced Neuronal Stress

MPP^+, 1-Methyl-4-phenylpyridinium iodide, (Sigma-Aldrich Corporation, St. Louis, MO, USA) was added at a concentration of 250 µM in PC12 and N27 cell lines and 300 µM in the SH-SY5Y cell line. The single compounds and combinations were administered for 24 hours post differentiation at 6 different concentrations: 1 nM, 10 nM, 100 nM, 1 µM, 10 µM and 100 µM.

Statistical Analysis

Data analyses performed using GraphPad Prism (GraphPad Software version 6.00. Inc., La Jolla, CA). Neurite length statistical comparison was performed using non-parametric Mann-Whitney Test. Neurite length was subjected to one-way ANOVA.

Pairwise comparisons for data quantification and significance were done using two-tailed Student's t-tests. (Significance: *P<0.05, **P<0.01, ***P<0.001). GraphPad Prism was used to graph dose-dependent response curves using parametric logistic algorism. Data was presented as mean ± SD.

Results

First the cells are differentiated using dibutyryl-cAMP, Nerve Growth Factor, Retinoic Acid, or TPA, respectively. Upon differentiation, the cells exhibit long, extended neurites. The long neurites allow the cells to communicate with neighboring cells and allow for synapses to occur. However, when we add methylglyoxal to the cell culture media, we see the methylglyoxal causes neuronal damage, characterized by retraction of neurites length **(Figure 5).** We randomly measured 100 neurites; only the length of one neurite was measured of each individual cell as traced with the red dotted line, using image J analysis **(Figure 6).**

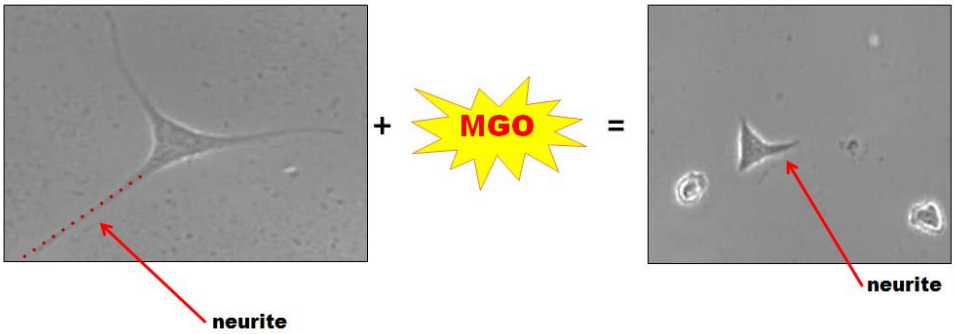

Figure 5: **Methylglyoxal-induced neuronal damage *in vitro*.**
Images of differentiated N27 cells exhibit long, extended neurites (red arrows). Administration of MGO causes retraction of neurite outgrowth and diminishes neuronal networks, as seen on far right image. (Image used from Sana Khateeb)

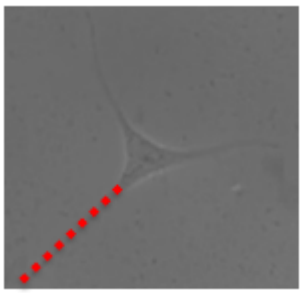

Figure 6: **Neurite length Quantification.**
Neurite (red dotted line) is defined as a thin projection longer than the diameter of the associate cell body is measured using Image J software. (Image used from Sana Khateeb)

A high-throughput drug screen was performed in *C. elegans* using supplement grade compounds to mitigate α-dicarbonyl levels. Using the same compounds examined in *C. elegans*, we validated their therapeutic efficacy *in vitro.* We tested the neuroprotective capacity of several supplement-grade compounds: B, Py, NA, N, VD, T, Py, L, A, and CA. There were 6 different concentrations used: 1nM, 10nM, 100nM, 1µM, 10µM and 100µM. We measured the therapeutic efficacy of each against 125 µM MGO at 0, 3, 6, 12 and 24 hours. All compounds administered at 12 and 24 hours showed effective rescue of neuronal damage. Ethanol was used as a vehicle control. When we used these supplement-grade compounds in the background of MGO stress, we saw that individual compounds work to ameliorate MGO neuronal damage. However, we see that the individual compounds never reached full rescue of the neurite length as compared to control at 12 and 24 hours **(Figure 7).** We then decided to combine two compounds to see whether the combinations can allow full recovery of the relative neurite length.

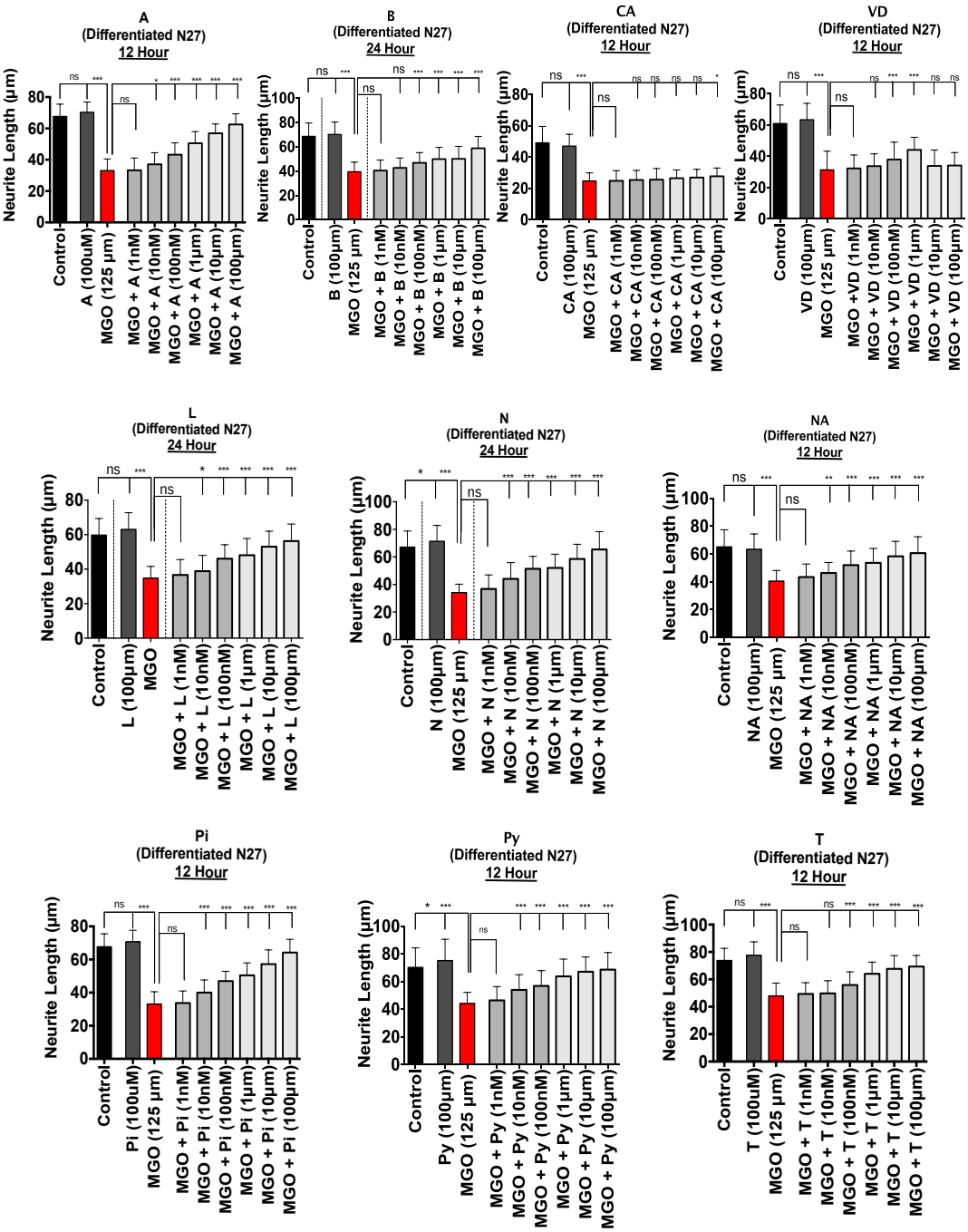

Figure 7: **Quantification of neuroprotective capacity against methylglyoxal-induced damage.**

Quantification of the single compounds: (A, B, CA, VD, L, N, NA, Pi, Py and T) therapeutic efficacy against MGO-induced neurotoxicity. Neurite length quantification in N27 neuronal cells, treated with EtOH or water (control), 125 µM MGO, and increasing concentrations (1nM, 10nM, 100 nM, 1 µM, 10 µM, or 100 µM) of single compounds + 125 µM MGO.

Using the compounds that were shown to have the most neuroprotective effect in our MGO-stress assay **(Figure 3)**, L, N and Py, we tested a total of four different combinations consisting of two compounds each. The combination included both compounds in a 1:1 ratio. The two compounds were used singly as a baseline control. The first combination of N+L was more effective than the L and N singles at every concentration, nearly reached full recovery at 10 µM. Py worked better than L and N did individually. The combination Py+N, was not able to enhance its efficacy; in fact it acted similarly to individual compounds. However, the combination of Py+L worked better than the two single compounds at every concentration except 10 µM **(Figure 8A).** A dose-response curve was generated relative to 125µM MGO neurite length **(Figure 8B).** From the two-compound combinations, we saw that L+N and Py+L worked best out of the three tested.

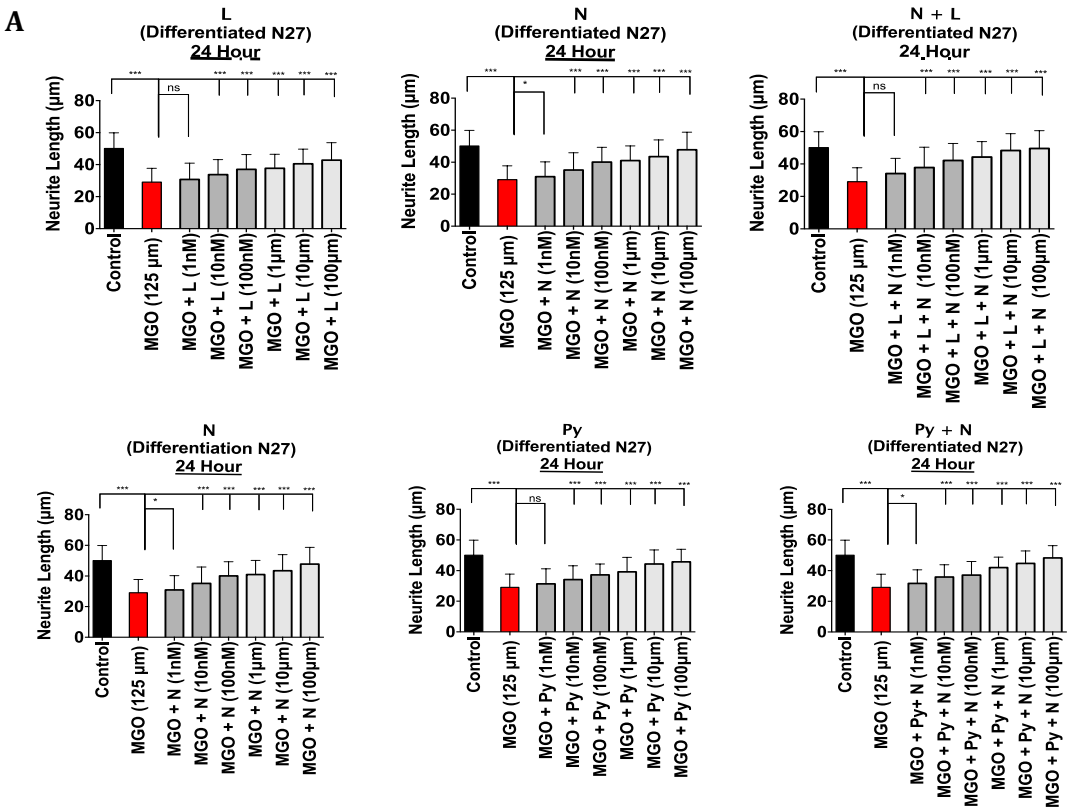

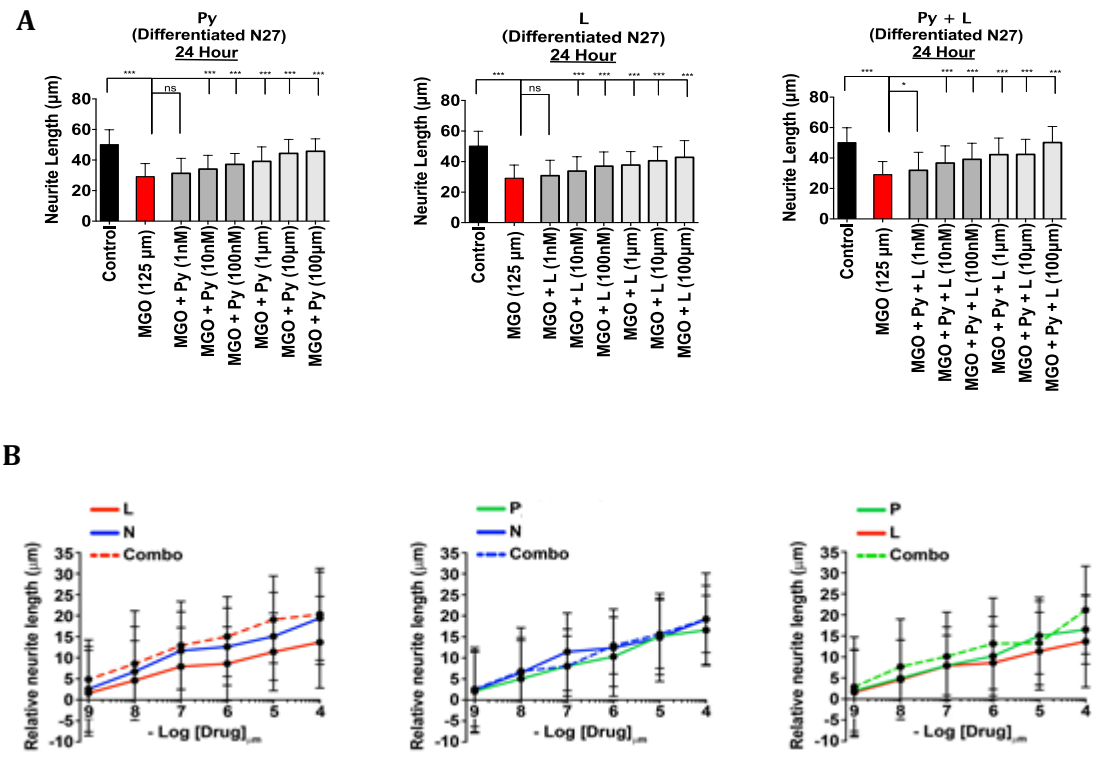

Figure 8: **Quantification of two-compound combination therapeutic capacity against MGO-induced toxicity.**
(A) Neurite length quantification in N27 cells, treated with EtOH/water (control), 125 µM MGO, and (1nM, 10nM, 100 nM, 1 µM, 10 µM, or 100 µM) compounds/combination +125 µM MGO.
(B) Dose response curves for neurite length relative to 125 µM MGO treated cells. In each graph, the dotted line represents the mixture of the two compounds and the solid line represents individual compounds, respectively.

From the three two-compound combinations we tested, the N+L mixture, and the L+Py mixture were the most effective two-compound combinations. We used L+N and Py+L as the combinations for a baseline to compare all the three-compound combinations. We tested several three-compound mixtures using a 1:1:1 ratio of each compound. We saw that neither (L+N+Ni) nor (L+N+A) worked as effectively as the L+N, two-compound, combination. When we observed the overall effectiveness of the

combination, we saw that L+N+Py and L+N+T were more effective than the two-compound combination at every concentration. When compared to L+Py, we see that most of the three-drug combinations worked similarly to the two-compound mixture, indicating that the three-compound mixtures were not enhancing its overall efficacy **(Figure 9A).** A dose response curve was generated relative to 125µM MGO neurite length **(Figure 9B).** Only the combinations of L+N+T and L+N+Py, worked more effectively than the double combination.

A

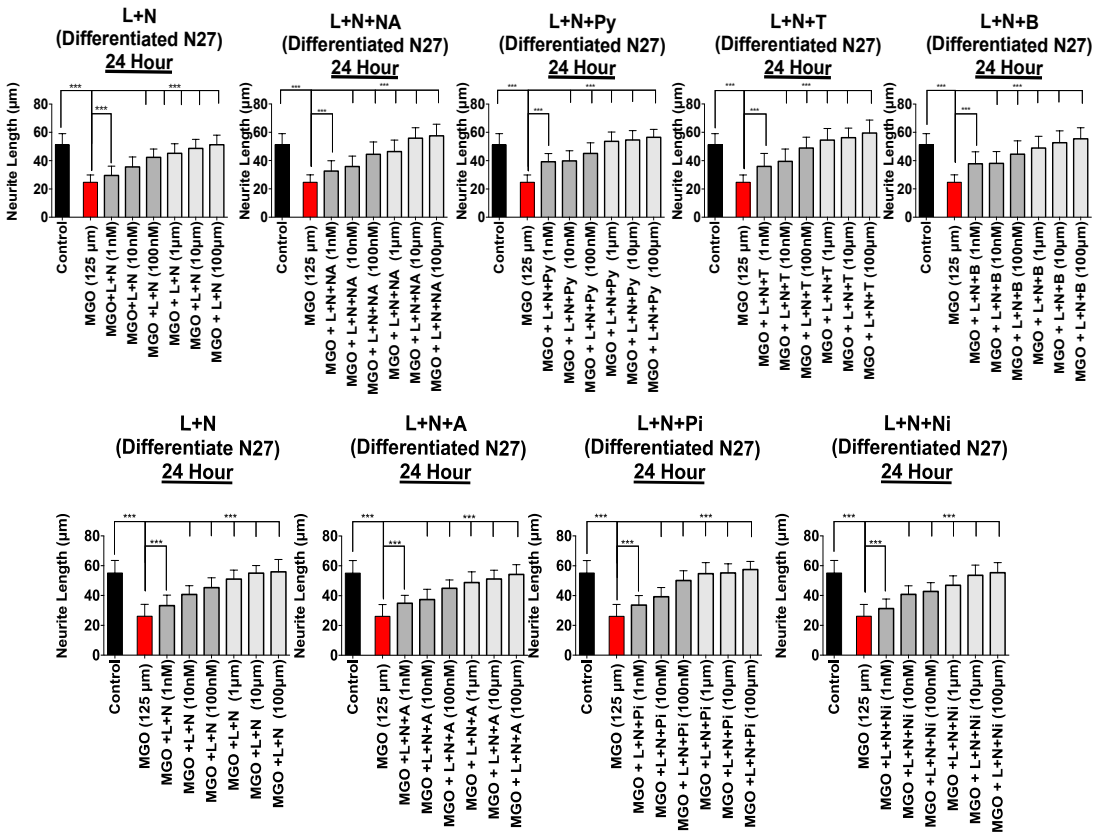

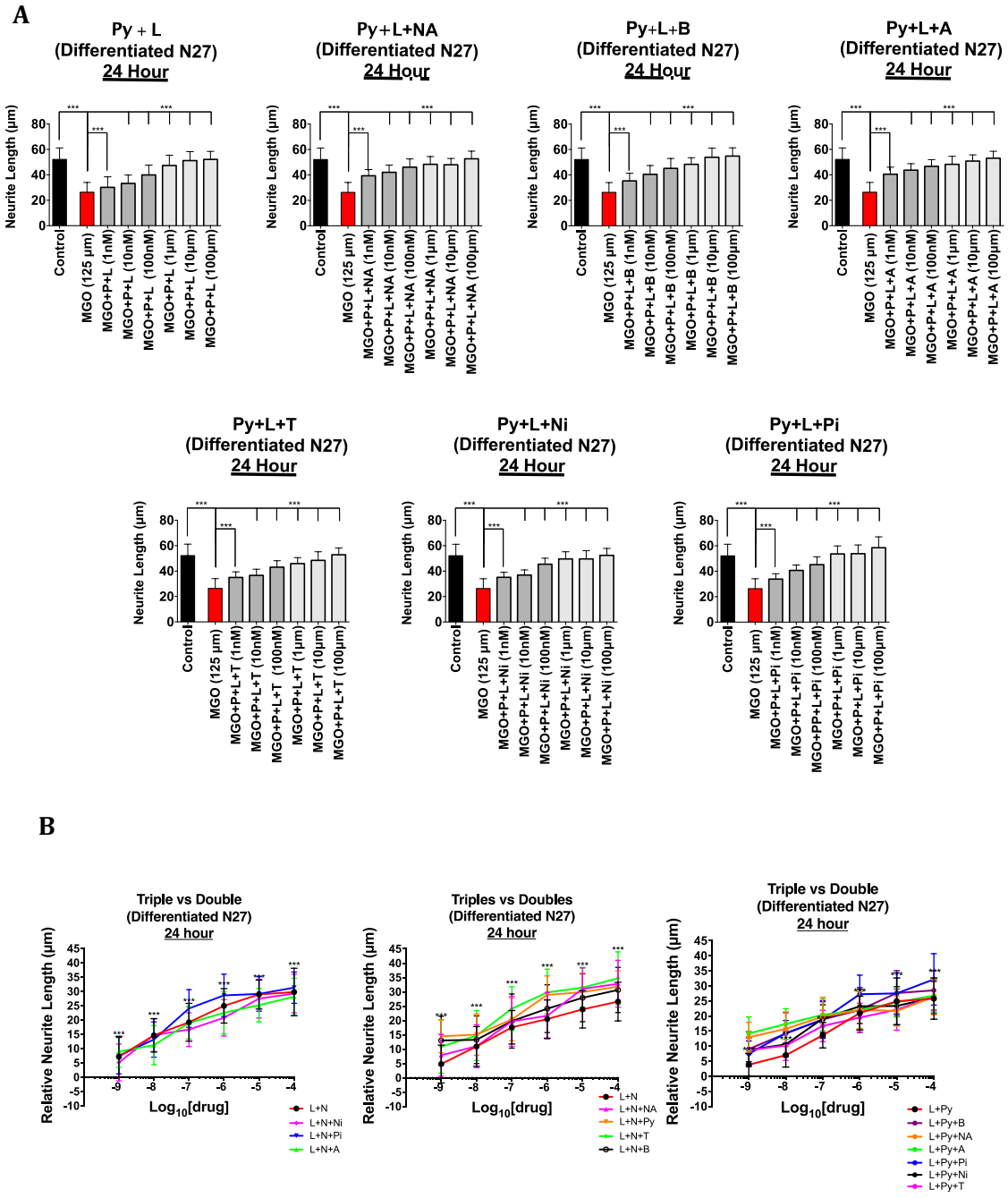

Figure 9: **Neuroprotective quantification of three-compound combination.**
(A) Neurite length quantification in N27 cells, treated with EtOH (control), 125 µM MGO, and (1nM, 10nM, 100 nM, 1 µM, 10 µM, or 100 µM) combination + 125 µM MGO.
(B) Dose response curves for neurite length relative to 125 µM MGO treated cells. In each graph, the red line represents the double combination (serving as a value for comparison) and the assorted color lines represent the different triple combinations.

From the 13 three-compound combinations we tested, we saw that the L+N+T mixture and the L+N+Py mixture were the more effective triple combinations at every concentration. We used L+N+T and L+N+Py to compare to our four-compound mixtures. We tested several four-compound mixtures using a 1:1:1:1 ratio of each compound. We see that at 1 nm and 10 nm the L+N+T+Pi combinations acts similar to the L+N+T combination. However, starting at 100 nm we see that the combination dramatically enhances the efficacy. And we see that the L+N+T+Py combination works similar to the three-compound mixture. Moreover, when we used L+N+Py as a control to test the other four-compound mixture, L+N+Py+Pi, we see that at the nM concentrations it in fact works less effective than the three-compound mixture, but starting at 1 µM it started to increase and work more effectively than the three-compound mixture **(Figure 10A).** A dose-response curve was generated relative to 125µM MGO neurite length **(Figure 10B).** We see that the combination of L, N, T and Pi worked more effectively than the L, N and T triple combination.

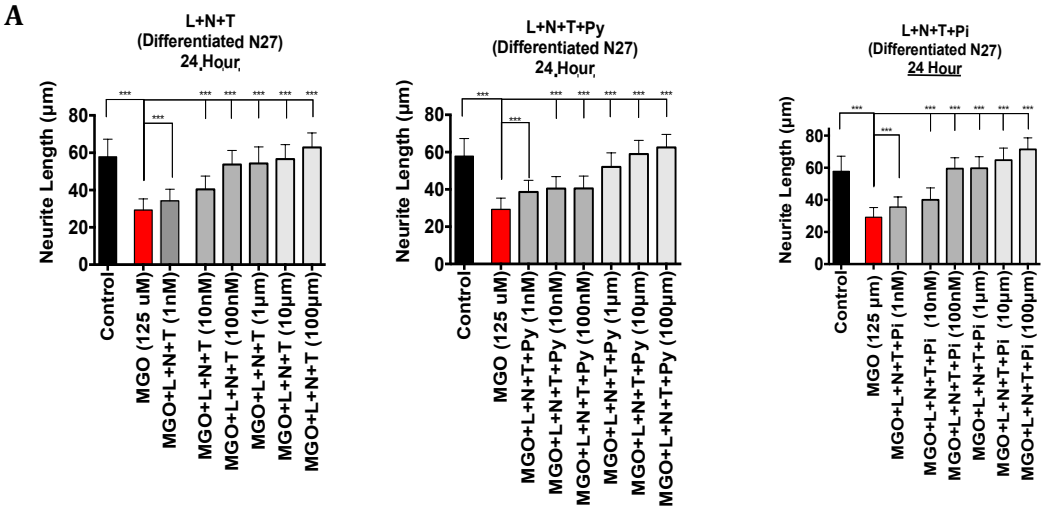

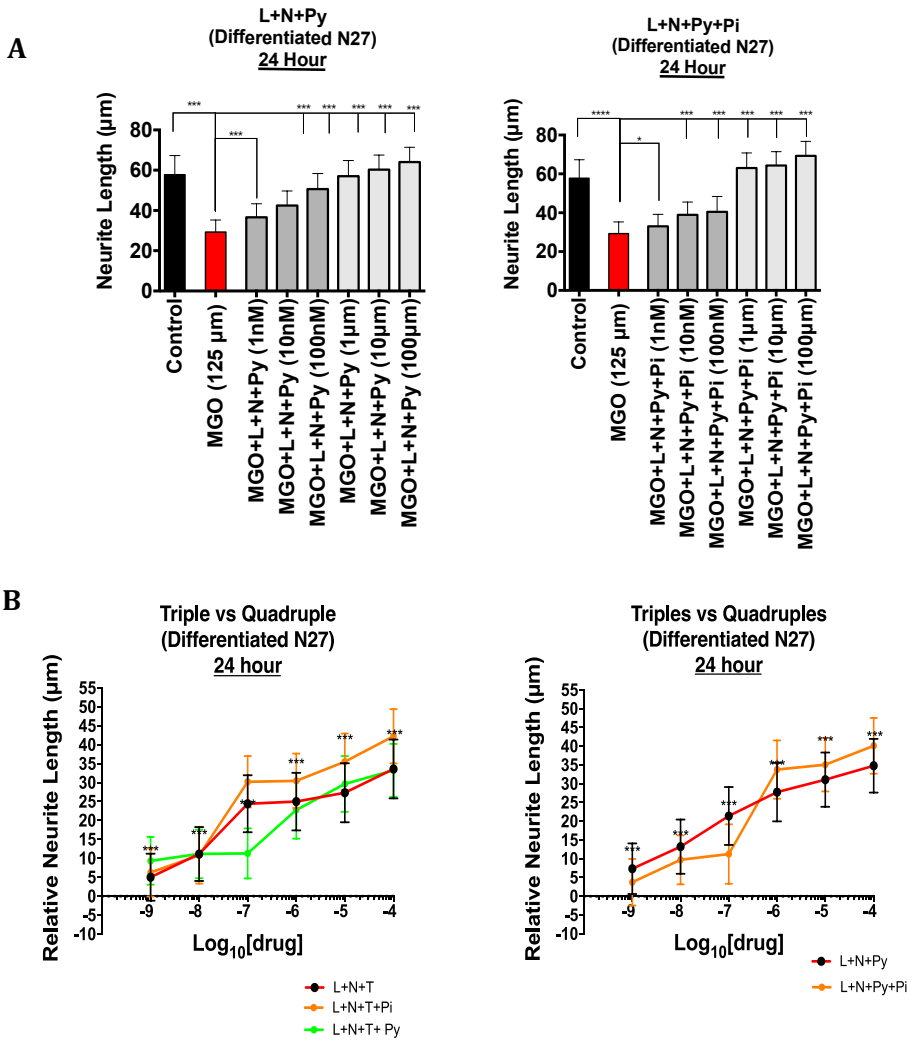

Figure 10: **Quantification of four-compound combination therapeutic capacity.** **(A)** Neurite length quantification in N27 dopaminergic neuronal cells, treated with EtOH (control), 125 µM MGO, and (1nM, 10nM, 100 nM, 1 µM, 10 µM, or 100 µM) combination + 125 µM MGO.
(B) Dose response curves for neurite length relative to 125 µM MGO treated cells. In each graph, the red line represents the triple combination (serving as a value for comparison) and the assorted colors represent the different quadruple combinations.

We used all three, four-compound mixtures to compare the efficacy of the five-compound mixtures. We saw that L+N+T+Py+Pi worked best to overcome MGO-induced neurotoxicity at low concentrations and we see a significant difference compared to the rest starting at 1 µM **(Figure 11A).** A dose-response curve was generated relative to 125µM MGO neurite length **(Figure 11B).** We saw that a five compound mixture

using a 1:1:1:1:1 ratio of L, N, T, Pi and Py worked more effectively than all the four-compound mixtures.

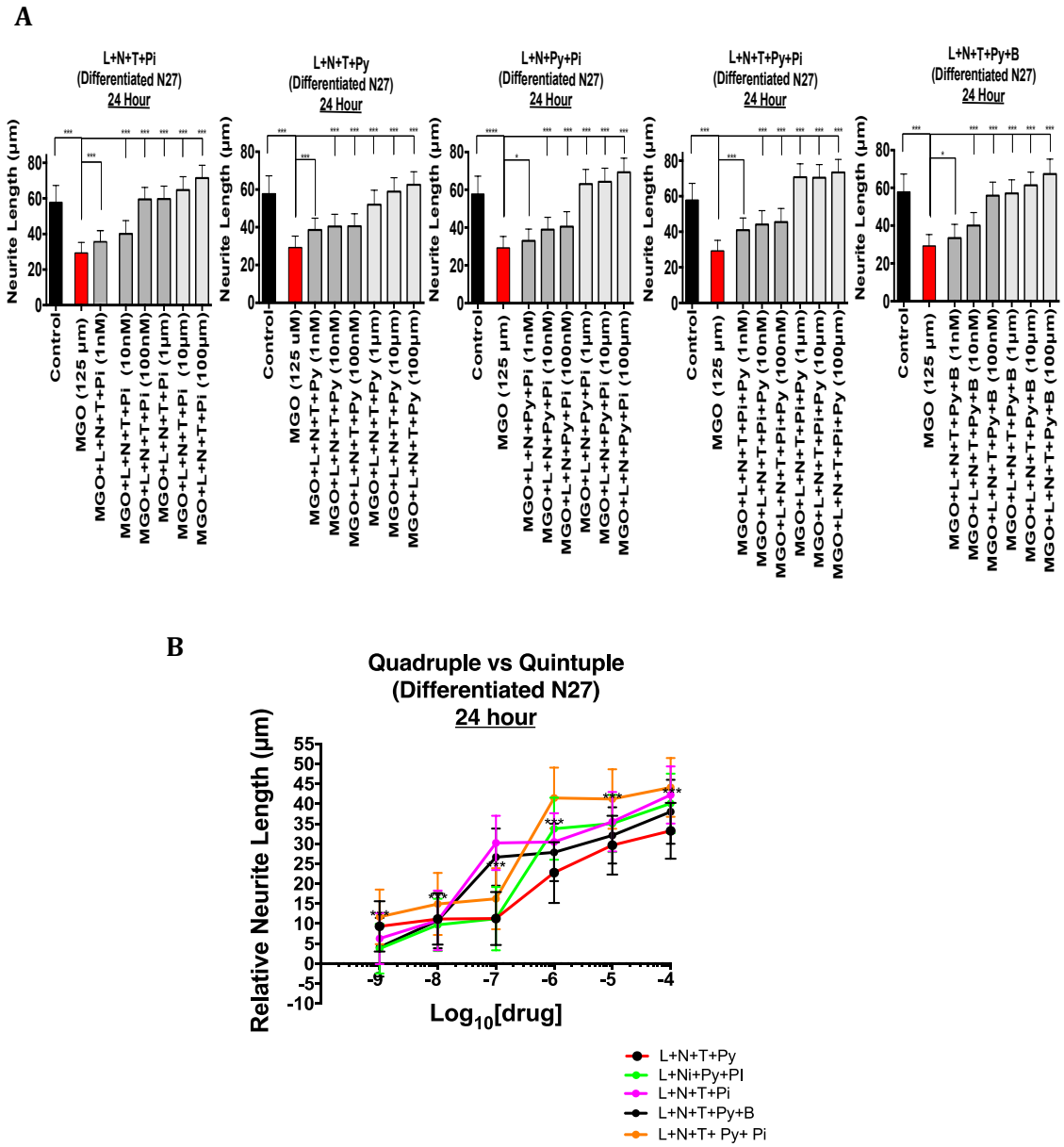

Figure 11: **Neuroprotective quantification of five-compound combination.**
(A) Neurite length quantification in rat dopaminergic neuronal cells, treated with EtOH (control), 125 µM MGO, and (1nM, 10nM, 100 nM, 1 µM, 10 µM, or 100 µM) combination + 125 µM MGO.
(B) Dose response curves for neurite length relative to 125 µM MGO treated cells. Red, green, and magenta lines represent the quadruple combinations (serving as values for comparison) and black and orange lines represent the two quintuple combinations, respectively.

Using this five-compound combination we decided to alter the amount of each compound we use in the mixture; essentially, increasing the amount of one compound while decreasing the amount of the remaining four compounds. We tested the 3:0.5:0.5:0.5:0.5 ratio combinations and compared them to 1:1:1:1:1 ratio five compound combinations. We saw that the LNTPyPi equal volumes worked almost the same as the (Pi)+L+N+T+Py, however, the altered combination with the increased amount of Pi worked better at lower concentrations, ultimately reaching a higher maximum value than the combination with equal amounts **(Figure 12A).** A dose response curve was generated relative to 125µM MGO neurite length **(Figure 12B).** We concluded that increasing the amount of Pi and equally decreasing the amount of L, T, N and Py showed a more therapeutic effect than equal amounts of L, N, T, Pi and Py.

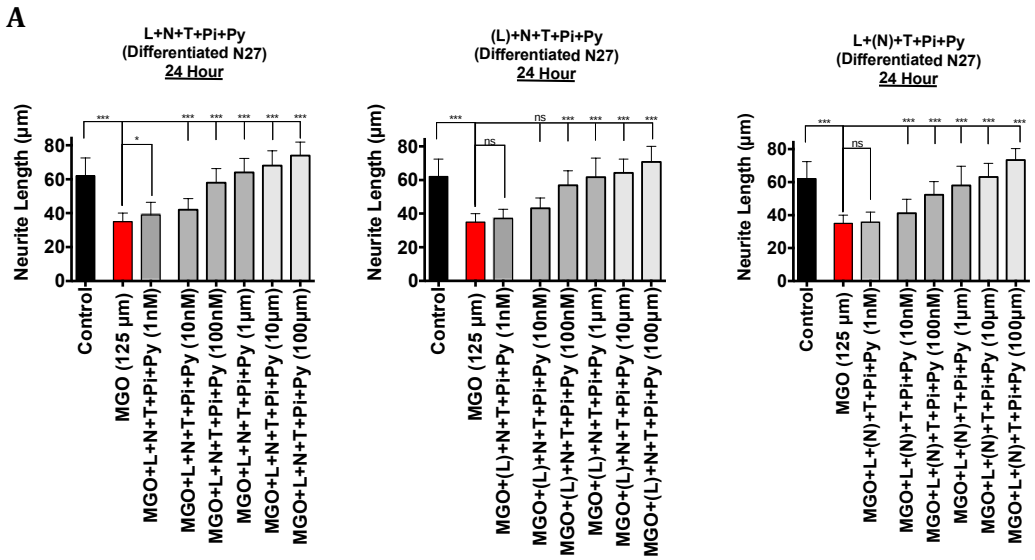

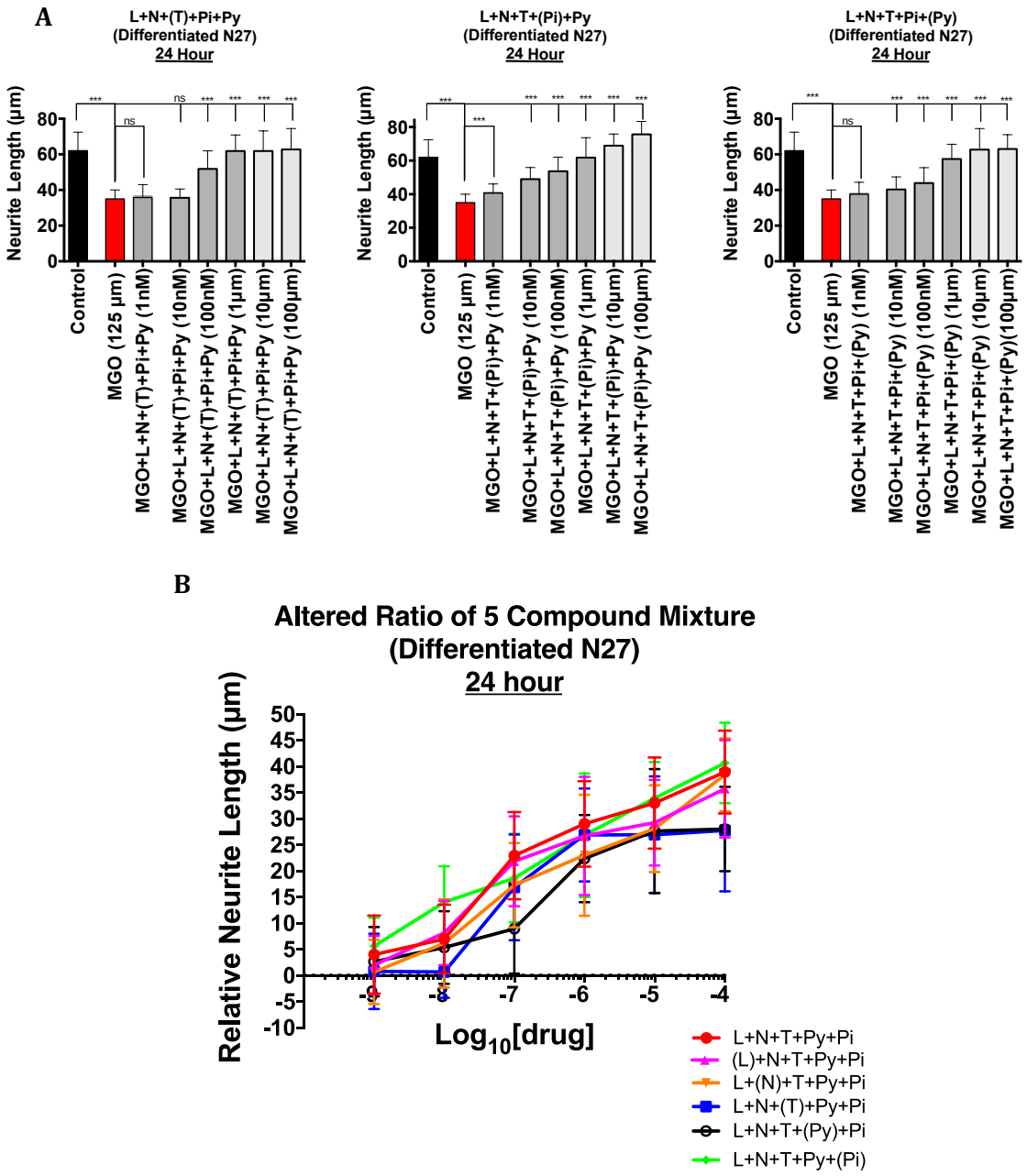

Figure 12: **Altered concentrations of each compound demonstrates a more effective approach at mitigating methylglyoxal-induced toxicity**
(A) Neurite length quantification in N27 cells treated with EtOH (control), 125 µM MGO, and (1nM, 10nM, 100 nM, 1 µM, 10 µM, or 100 µM) combination + 125 µM MGO.
(B) Dose response curves for neurite length relative to 125 µM MGO treated cells. The red line represents the five-compound combination with equal concentrations of each compound. The assorted color lines represent the combination with altered concentrations, parenthesis indicate which compound was altered.

We saw that the two, five-compound mixtures worked really well to alleviate MGO stress in the N27 cell line, so, we wanted to test this phenomenon in different dopaminergic cell lines: PC12 and SH-SY5Y. When we tested the equal ratio combination and the best-altered ratio combination, increased amount of Pi, in the PC12 cell line, we saw that at 1 µM the L+N+T+Py+(Pi) combination was more effective than the L+N+T+Py+Pi combination that was comprised of equal volumes of each compound. When we tested these two different five-compound combinations in the human cell line, SH-SY5Y, we saw that at 100 nM the altered mix, L+N+T+Py+(Pi), works better than the compound with equal volumes **(Figure 13A).** A dose response curve was generated relative to 125µM MGO neurite length **(Figure 13B).** We saw that these combinations worked to rescue MGO-induced neuronal damage in both PC12 and SH-SY5Y cell lines.

A

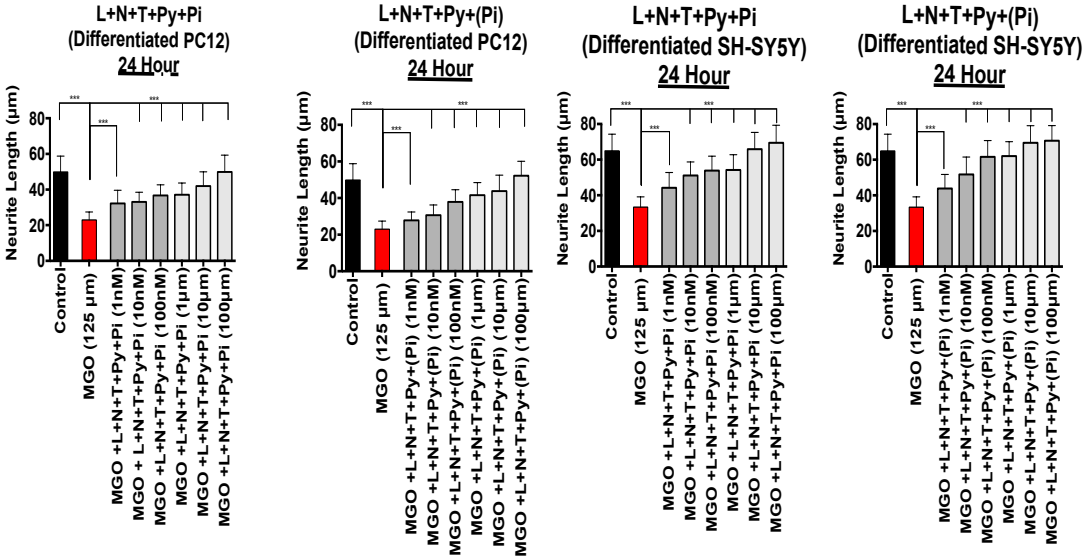

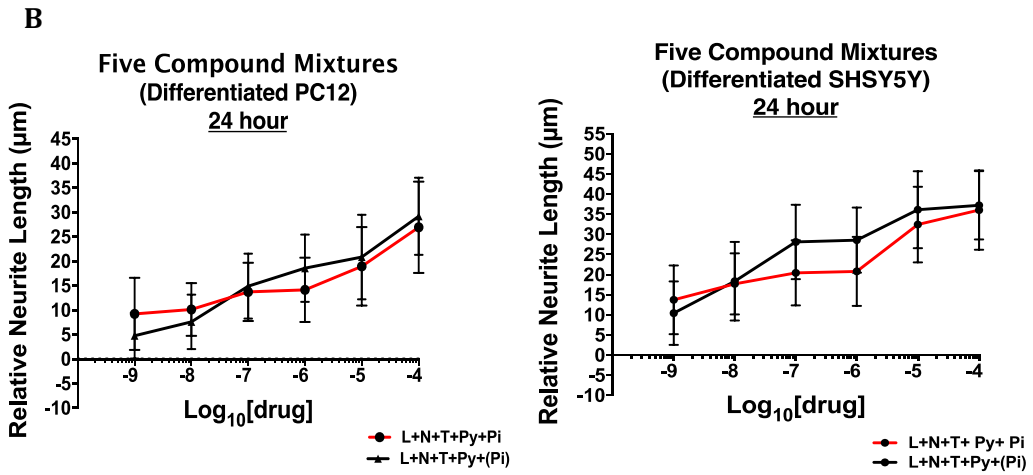

Figure 13: **Five-compound mixtures counteract methylglyoxal-induced cellular damage in PC12 and SH-SY5Y cell lines.**
(A) Neurite length quantification in rat/human dopaminergic neuronal cells, treated with EtOH (control), 125/250 µM MGO, and (1nM, 10nM, 100 nM, 1 µM, 10 µM, or 100 µM) combination + 125/250 µM MGO.
(B) Dose response curves for neurite length relative to 125/250 µM MGO treated cells. In each graph, the red line represents the five-compound combination with equal concentrations of each compound and the black line represents the combination with increased concentration of Pi

We compared the singles, L and N, to the two different five-compound combinations, LNTPyPi and LNTPy(Pi), in three different dopaminergic cell lines, under both MGO and MPP+ stress. We see that in the PC12 cell line, the two, five-compound mixtures surpass the control value at 1µM and under MPP+ it reached the control value at 10 µM. We then used the two best five compound mixtures and compared their neuroprotective capacity with the two best individual compounds **(Figure 14A).** All four mixtures were tested under MGO-induced neurotoxicity and MPP^+-induced neurotoxicity. We see that the two compounds alone do not fully rescue MGO and MPP^+-induced stress as compared to the control neurite length. However, the two mixtures fully rescue MGO and MPP^+-induced stress at lower concentrations, starting at 1 µM **(Figure 14B).**

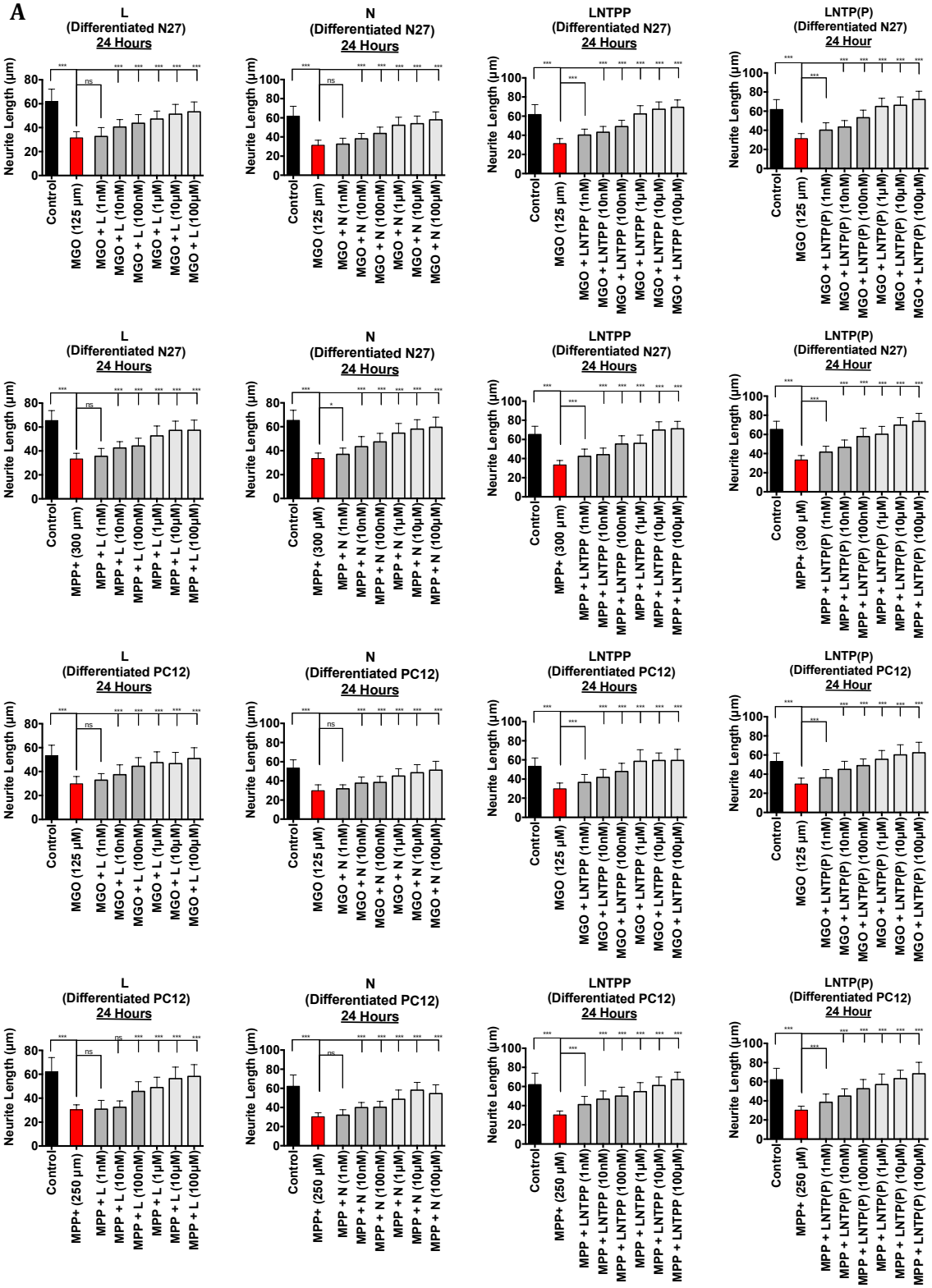
A
L
(Differentiated N27)
24 Hours
N
(Differentiated N27)
24 Hours
LNTPP
(Differentiated N27)
24 Hours
LNTP(P)
(Differentiated N27)
24 Hour
L
(Differentiated N27)
24 Hours
N
(Differentiated N27)
24 Hours
LNTPP
(Differentiated N27)
24 Hours
LNTP(P)
(Differentiated N27)
24 Hour
L
(Differentiated PC12)
24 Hours
N
(Differentiated PC12)
24 Hours
LNTPP
(Differentiated PC12)
24 Hours
LNTP(P)
(Differentiated PC12)
24 Hour
L
(Differentiated PC12)
24 Hours
N
(Differentiated PC12)
24 Hours
LNTPP
(Differentiated PC12)
24 Hours
LNTP(P)
(Differentiated PC12)
24 Hour
Neurite Length (µm)
Control
MGO (125 µm)
MGO + L (1nM)
MGO + L (10nM)
MGO + L (100nM)
MGO + L (1µM)
MGO + L (10µM)
MGO + L (100µM)
MGO + N (1nM)
MGO + N (10nM)
MGO + N (100nM)
MGO + N (1µM)
MGO + N (10µM)
MGO + N (100µM)
MGO + LNTPP (1nM)
MGO + LNTPP (10nM)
MGO + LNTPP (100nM)
MGO + LNTPP (1µM)
MGO + LNTPP (10µM)
MGO + LNTPP (100µM)
MGO + LNTP(P) (1nM)
MGO + LNTP(P) (10nM)
MGO + LNTP(P) (100nM)
MGO + LNTP(P) (1µM)
MGO + LNTP(P) (10µM)
MGO + LNTP(P) (100µM)
MPP+ (300 µM)
MPP + L (1nM)
MPP + L (10nM)
MPP + L (100nM)
MPP + L (1µM)
MPP + L (10µM)
MPP + L (100µM)
MPP+ (300 µM)
MPP + N (1nM)
MPP + N (10nM)
MPP + N (100nM)
MPP + N (1µM)
MPP + N (10µM)
MPP + N (100µM)
MPP + LNTPP (1nM)
MPP + LNTPP (10nM)
MPP + LNTPP (100nM)
MPP + LNTPP (1µM)
MPP + LNTPP (10µM)
MPP + LNTPP (100µM)
MPP + LNTP(P) (1nM)
MPP + LNTP(P) (10nM)
MPP + LNTP(P) (100nM)
MPP + LNTP(P) (1µM)
MPP + LNTP(P) (10µM)
MPP + LNTP(P) (100µM)
MGO (125 µM)
MPP+ (250 µM)

A

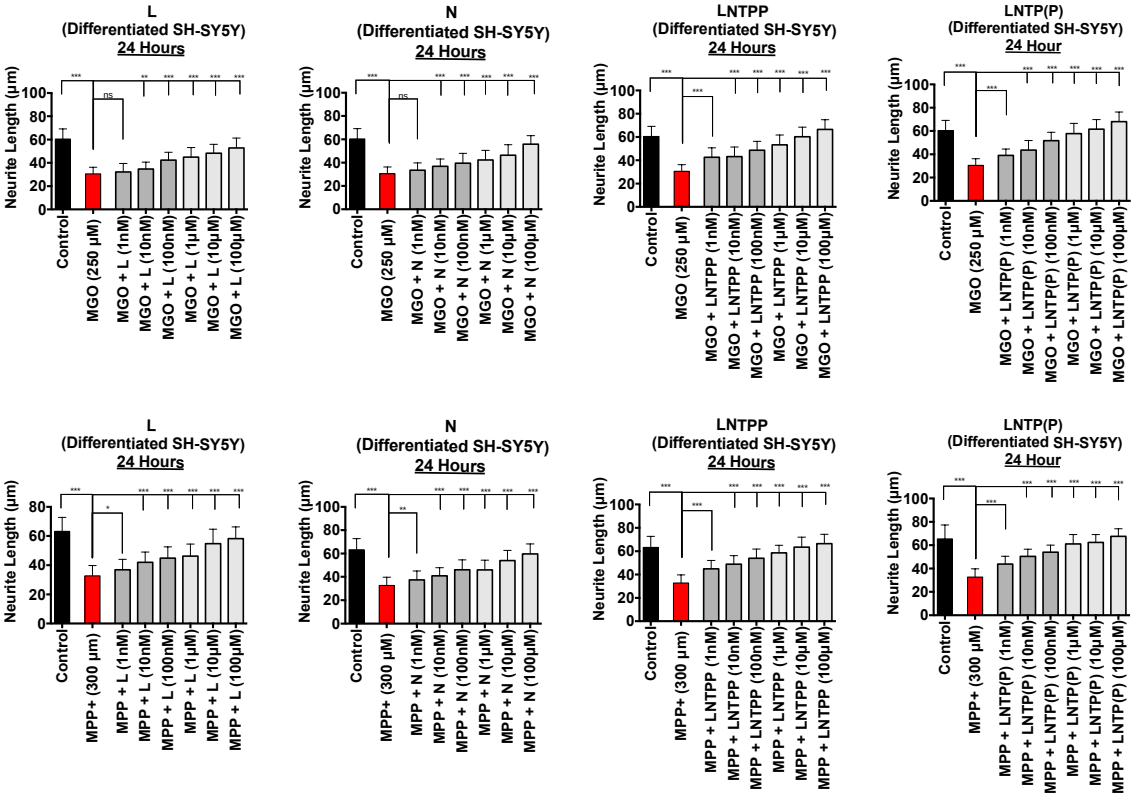
L
(Differentiated SH-SY5Y)
24 Hours
N
(Differentiated SH-SY5Y)
24 Hours
LNTPP
(Differentiated SH-SY5Y)
24 Hours
LNTP(P)
(Differentiated SH-SY5Y)
24 Hour
Neurite Length (µm)
Control
MGO (250 µM)
MGO + L (1nM)
MGO + L (10nM)
MGO + L (100nM)
MGO + L (1µM)
MGO + L (10µM)
MGO + L (100µM)
MGO + N (1nM)
MGO + N (10nM)
MGO + N (100nM)
MGO + N (1µM)
MGO + N (10µM)
MGO + N (100µM)
MGO + LNTPP (1nM)
MGO + LNTPP (10nM)
MGO + LNTPP (100nM)
MGO + LNTPP (1µM)
MGO + LNTPP (10µM)
MGO + LNTPP (100µM)
MGO + LNTP(P) (1nM)
MGO + LNTP(P) (10nM)
MGO + LNTP(P) (100nM)
MGO + LNTP(P) (1µM)
MGO + LNTP(P) (10µM)
MGO + LNTP(P) (100µM)
L
(Differentiated SH-SY5Y)
24 Hours
N
(Differentiated SH-SY5Y)
24 Hours
LNTPP
(Differentiated SH-SY5Y)
24 Hours
LNTP(P)
(Differentiated SH-SY5Y)
24 Hour
MPP+ (300 µm)
MPP + L (1nM)
MPP + L (10nM)
MPP + L (100nM)
MPP + L (1µM)
MPP + L (10µM)
MPP + L (100µM)
MPP + N (1nM)
MPP + N (10nM)
MPP + N (100nM)
MPP + N (1µM)
MPP + N (10µM)
MPP + N (100µM)
MPP + LNTPP (1nM)
MPP + LNTPP (10nM)
MPP + LNTPP (100nM)
MPP + LNTPP (1µM)
MPP + LNTPP (10µM)
MPP + LNTPP (100µM)
MPP + LNTP(P) (1nM)
MPP + LNTP(P) (10nM)
MPP + LNTP(P) (100nM)
MPP + LNTP(P) (1µM)
MPP + LNTP(P) (10µM)
MPP + LNTP(P) (100µM)

B

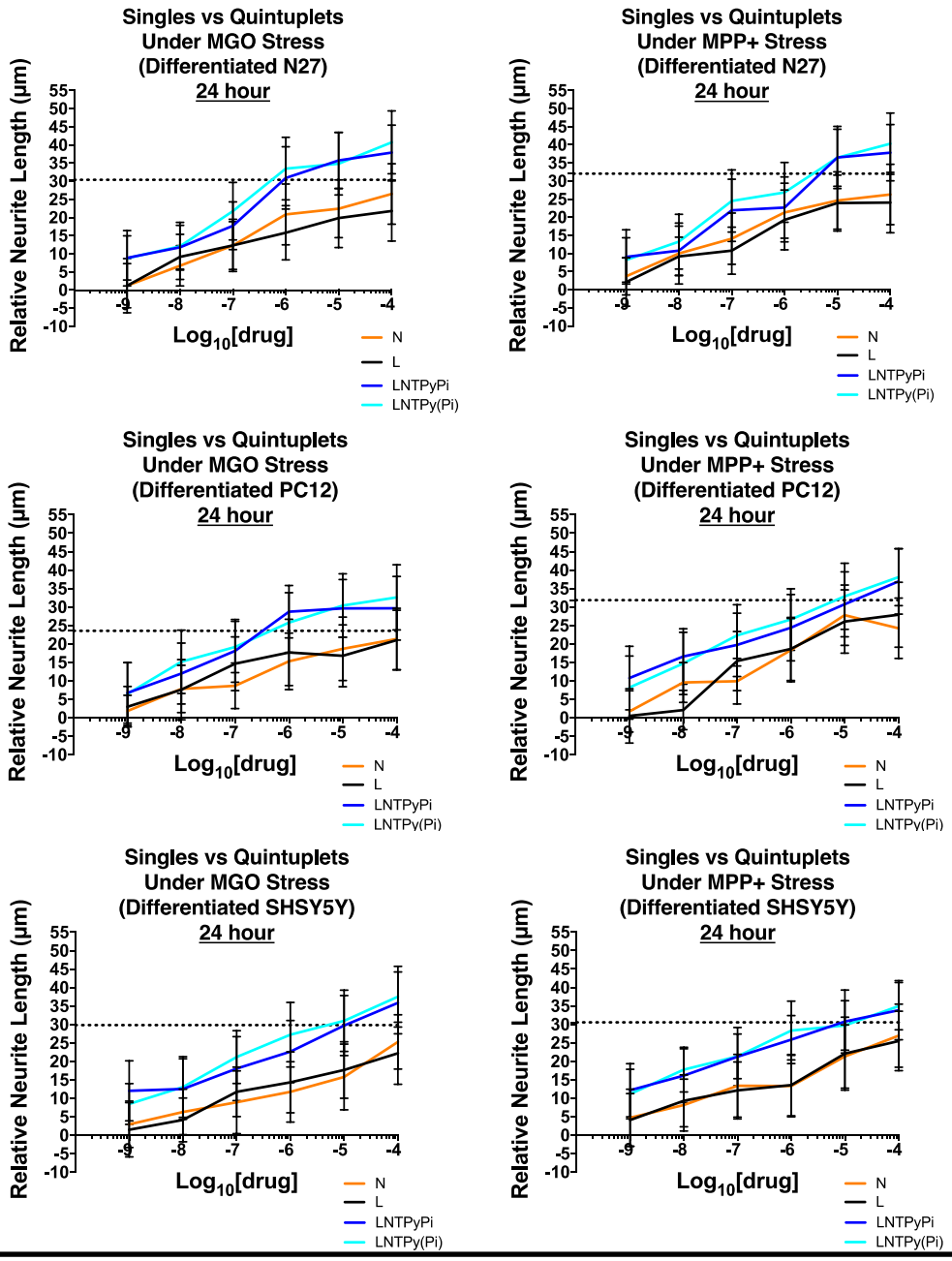

***Figure 14*: Five-compound combinations versus single compound under methylglyoxal and MPP^+ induced neurotoxicity.**

(A) Neurite length quantification in rat/human dopaminergic neuronal cells, treated with EtOH (control), 125/250 µM MGO or 250/300 µM MPP^+, and (1nM, 10nM, 100 nM, 1 µM, 10 µM, or 100 µM) compounds/combination + 125/250 µM MGO or 250/300 µM MPP^+

(B) Dose response curves for neurite length relative to 125/250 µM MGO or 250/300 µM MPP^+, treated cells. Dotted line represents the relative neurite length of control (untreated) cells. The orange and black lines represent the single compounds, respectively. The dark and light blue lines represent the two different five-compound mixtures, respectively.

In addition to the single compounds, D and P were compounds that also came out of the previous drug screen using *C. elegans* and were tested on other cell lines that worked to alleviate MGO-induced damage (data not shown). Efficacy of the two single compounds, D and P, was compared to the two five-compound combinations, LNTPyPi and LNTPy(Pi), against MGO and MPP^+ stress in 3 different dopaminergic cell lines **(Figure 15 A).** We saw the D and P work to rescue MGO and MPP^+ neuronal damage. We see that under MGO stress in N27 and PC12 cell lines, PA works very similar to LNTPyPi. However, under all conditions examined we ultimately see that the two five-compound mixtures works more effectively at overcoming MGO and MPP^+ neuronal stress than both the two single compounds **(Figure 15 B).**

A

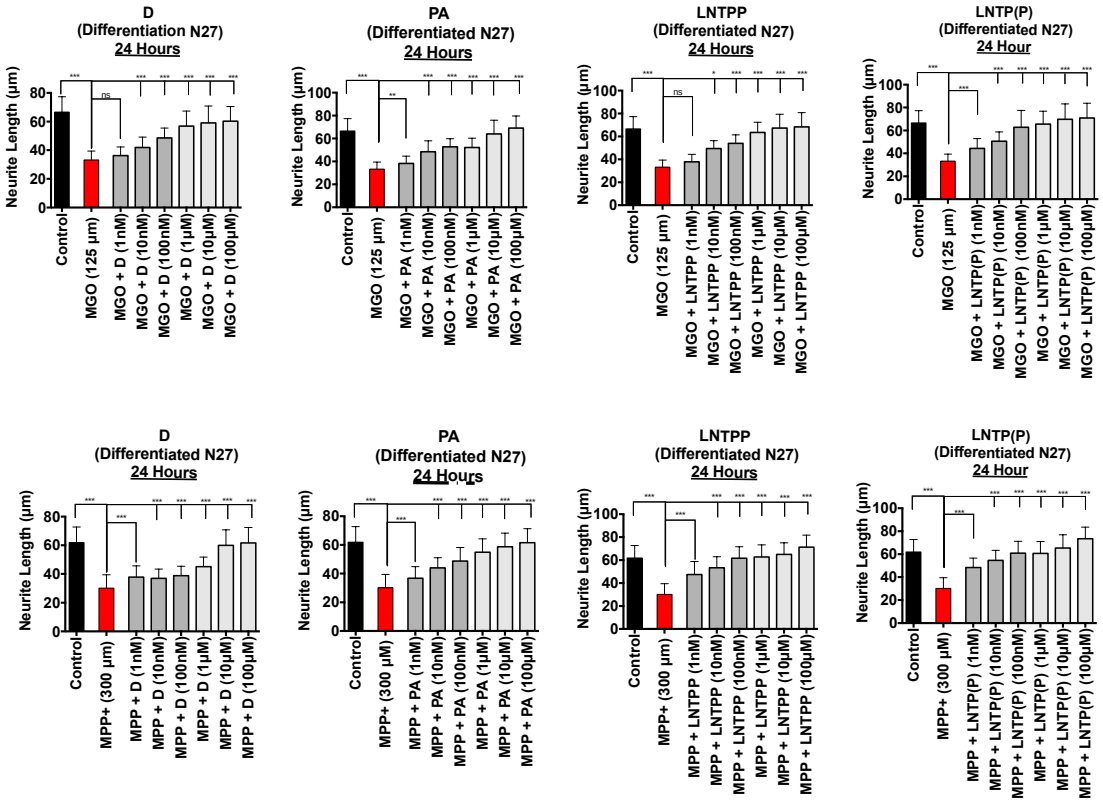

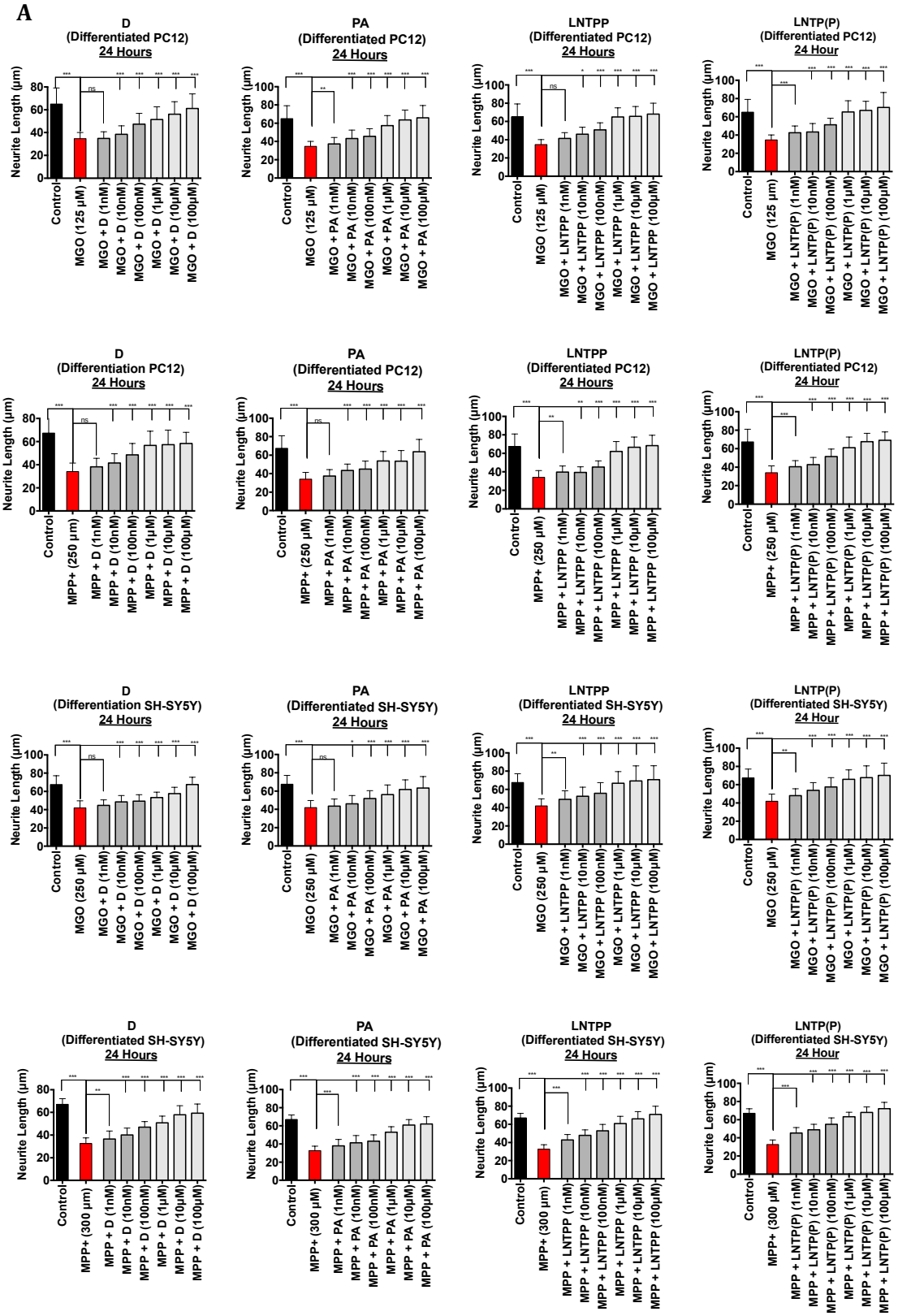
A
D
(Differentiated PC12)
24 Hours
PA
(Differentiated PC12)
24 Hours
LNTPP
(Differentiated PC12)
24 Hours
LNTP(P)
(Differentiated PC12)
24 Hour
D
(Differentiation PC12)
24 Hours
PA
(Differentiated PC12)
24 Hours
LNTPP
(Differentiated PC12)
24 Hours
LNTP(P)
(Differentiated PC12)
24 Hour
D
(Differentiation SH-SY5Y)
24 Hours
PA
(Differentiated SH-SY5Y)
24 Hours
LNTPP
(Differentiated SH-SY5Y)
24 Hours
LNTP(P)
(Differentiated SH-SY5Y)
24 Hour
D
(Differentiated SH-SY5Y)
24 Hours
PA
(Differentiated SH-SY5Y)
24 Hours
LNTPP
(Differentiated SH-SY5Y)
24 Hours
LNTP(P)
(Differentiated SH-SY5Y)
24 Hour
Neurite Length (µm)
Control
MGO (125 µM)
MGO + D (1nM)
MGO + D (10nM)
MGO + D (100nM)
MGO + D (1µM)
MGO + D (10µM)
MGO + D (100µM)
MGO + PA (1nM)
MGO + PA (10nM)
MGO + PA (100nM)
MGO + PA (1µM)
MGO + PA (10µM)
MGO + PA (100µM)
MGO + LNTPP (1nM)
MGO + LNTPP (10nM)
MGO + LNTPP (100nM)
MGO + LNTPP (1µM)
MGO + LNTPP (10µM)
MGO + LNTPP (100µM)
MGO + LNTP(P) (1nM)
MGO + LNTP(P) (10nM)
MGO + LNTP(P) (100nM)
MGO + LNTP(P) (1µM)
MGO + LNTP(P) (10µM)
MGO + LNTP(P) (100µM)
MPP+ (250 µM)
MPP + D (1nM)
MPP + D (10nM)
MPP + D (100nM)
MPP + D (1µM)
MPP + D (10µM)
MPP + D (100µM)
MPP + PA (1nM)
MPP + PA (10nM)
MPP + PA (100nM)
MPP + PA (1µM)
MPP + PA (10µM)
MPP + PA (100µM)
MPP + LNTPP (1nM)
MPP + LNTPP (10nM)
MPP + LNTPP (100nM)
MPP + LNTPP (1µM)
MPP + LNTPP (10µM)
MPP + LNTPP (100µM)
MPP + LNTP(P) (1nM)
MPP + LNTP(P) (10nM)
MPP + LNTP(P) (100nM)
MPP + LNTP(P) (1µM)
MPP + LNTP(P) (10µM)
MPP + LNTP(P) (100µM)
MPP+ (300 µM)

B

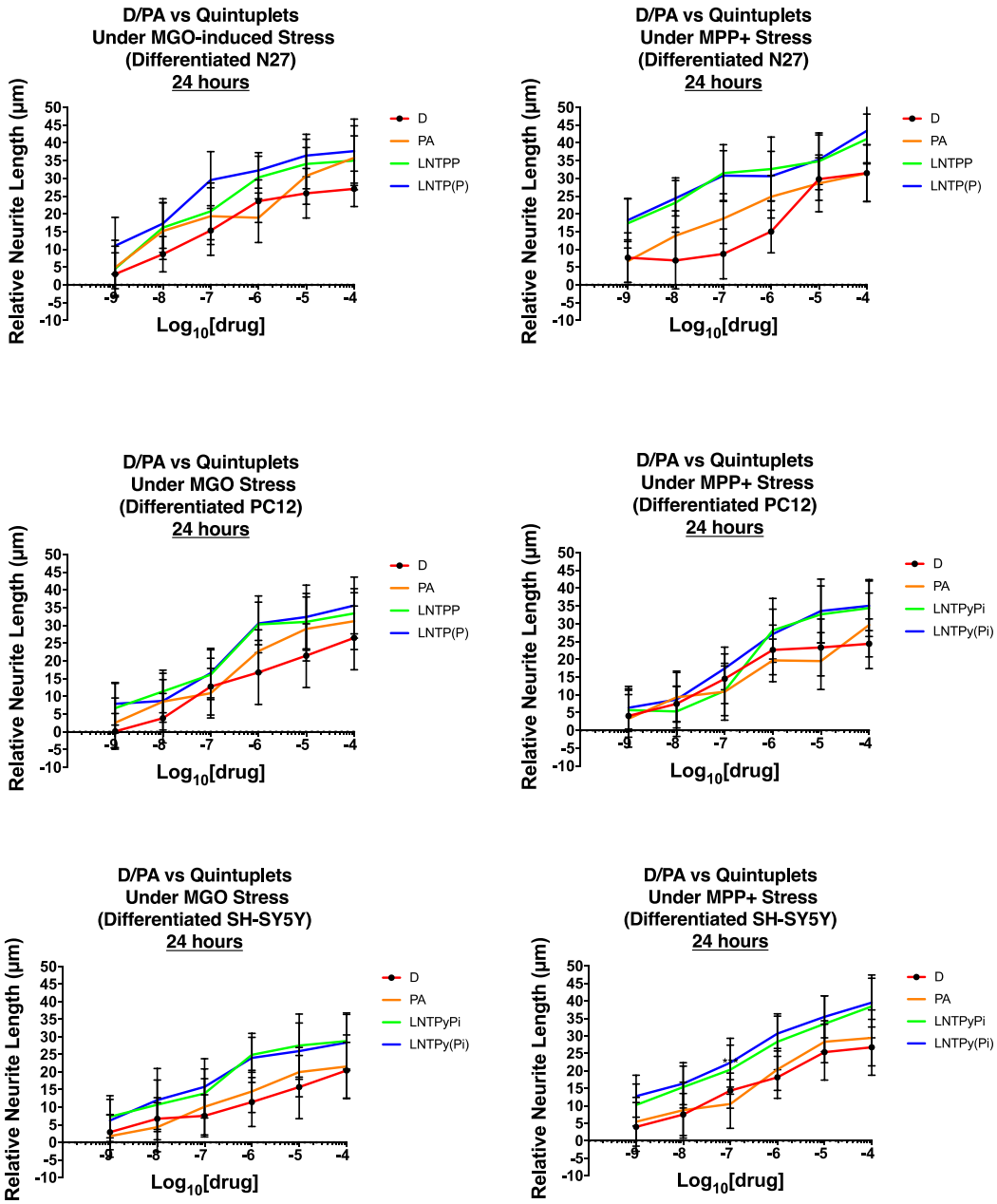

Figure 15: **Combinational and monotherapy against MGO and MPP$^+$-induced neurotoxicity.**

(A) Neurite length quantification in rat/human dopaminergic neuronal cells, treated with EtOH (control), 125/250 µM MGO or 250/300 µM MPP$^+$, and (1nM, 10nM, 100 nM, 1 µM, 10 µM, or 100 µM) compounds/combination + 125/250 µM MGO or 250/300 µM MPP$^+$

(B) Dose response curves for neurite length relative to 125/250 µM MGO or 250/300 µM MPP$^+$, treated cells. On each of the graphs, the red and orange lines represent the single compounds and the blue and green lines represent the two five-compound combinations, respectively.

Discussion

Hyperglycemia and oxidative stress produce toxic byproducts known as, α-dicarbonyls, which are linked to the pathogenesis of diabetes. High α-dicarbonyls levels give rise to advanced glycation end products (AGEs), which seems to be the etiology agent of secondary diabetic complications and neurodegenerative disorders such as Parkinson's disease. AGEs and their precursors, α-dicarbonyls, are the subject of studies focusing on understanding their influence on the progression of aging and age-associated disease. The accumulation of AGEs and the biochemical mechanism as to how they are sensed, formed, and detoxified is a major bottleneck in understanding AGEs-related pathologies. Our understanding of α-dicarbonyls and AGEs has permitted the development of several therapeutic agents. Numerous natural compounds were screened for TRPA-1-Nrf2 inducer activity in *Caenorhabditis elegans*. The drug screen revealed several supplement grade compounds that decreased α-dicarbonyls (e.g. methylglyoxal/MGO) levels utilizing the TRPA-1-Nrf-2 pathway (6). We see that the compounds worked effectively in *C. elegans* and we went on to test their therapeutic efficacy through mammalian *in vitro* studies. Studying the compound's rescuing effects can help us develop a therapeutic reagent that protects against neurotoxicity.

We test these compounds to rescue methylglyoxal-induced cellular damage, ultimately to prevent the accumulation of AGEs, which seem to be synergistic with pathogenic pathways in diabetes. In this study, we focus on methylglyoxal detoxification as the therapeutic target. These supplements exert very powerful protective effects, allowing us to use these compounds as potential supplement to hinder the progression of diabetes and/or Parkinson's disease.

Validate individual candidates from drug screen in mammalian cell culture.

Previous worm findings emphasized the need for mammalian *in vitro* studies, to validate various supplement-grade compounds in the background of methylglyoxal stress and test their neuroprotective capacity in preventing neurite retraction caused by methylglyoxal. We identified eight compounds that were protective against methylglyoxal-induced neurotoxicity. Quantifying the neurite length of each cell post drug administration, we saw that most compounds rescued the neurite retraction caused by methylglyoxal within 12 to 24 hours. However, our results show that VD and CA did not work to rescue methylglyoxal cellular damage. Although these compounds worked well in worms we did not see the same beneficial effect in cell culture. We might not have seen the same effect in cell culture because this process is likely not completely conserved between worms and cells, therefore, some differences could be expected.

While our worm data suggests that each compound ultimately bolsters methylglyoxal detoxification, they target different parts of the TRPA-1-Nrf2 pathway that regulate methylglyoxal detoxification. So, instead of pursuing individual compounds, we decided to test various combinations. Some compounds activate SKN1/Nrf-2 both independent of and dependent on TRPA-1 suggesting that the compound provides a better outcome due to possible crosstalk to synergistically upregulate the glyoxalase for functional detoxification of methylglyoxal.

Test various combinations to identify a more effective approach in ameliorating methylglyoxal stress.

Our goal was to find a unique mixture, by combining the most effective compounds in order to identify a combination that will ameliorate methylglyoxal toxicity

more effectively than single compounds. Clinical trials have demonstrated that a single compound was ineffective at reducing methylglyoxal levels, however, compounds given in combination showed clearance of methylglyoxal in the plasma of patients (55). Similar to what they have shown, we tested several combinations in mammalian *in vitro* studies, and we saw that the single compounds never fully rescued the length of the neurite as compared to the combinations. Our results showed that when we added five different compounds to the mixture not only did we achieve full rescue but the neurite length was phenotypically better than the control, indicating that the mixture exhibited robust effects. We showed that after meticulously testing many binary, ternary, quaternary combinations, the five-compound mixture, which includes L, N, T, Pi, and Py, was most effective in ameliorating methylglyoxal-induced stress. We believe that the five-compound combination enhanced the effectiveness as compared to the other combinations we tested because of the addition of Py to the mixture. The Py compound acts as α-dicarbonyl scavenger, ultimately inhibiting the formation of AGEs (53), therefore, we believe that the addition of this specific compound enhanced its overall potency and efficacy, making it the best combination we tested thus far. This data showed us that with combinational therapy we were able to successfully counter-act methylglyoxal damage. This combination may target an uncharacterized pathway to activate either of the glyoxalases, which may be lowering levels of methylglyoxal that will simultaneously prevent formation of methylglyoxal-derived AGEs.

In the L+N+T+Py+Pi mixture, we saw that even at the lowest concentration of the mixture (1 nM), which included only 200 pM concentration of each individual drug; the mix resulted in significant improvement. It is to our surprise that, in generating this

mixture, we effectively reduced each of the individual compounds concentration by 5 folds, while increasing the overall effectiveness of the treatment (see Figure 11). We worked out dosages where we saw that the combination worked at lower concentrations and at the maximum effect it worked better than the control. Results suggest that this combination can potentially be used as a supplement, reducing the amount of multiple agents without undermining the suitable outcome, thereby, minimizing the risk of probable side effects. Given evidence that some of the compounds within our mixture inhibit glycation, one possible explanation for this effect is inactivating and trapping methylglyoxal and consequently reducing methylglyoxal stress (53). Each of the compounds possesses antioxidant, scavenging, and neuroprotective properties, suggesting that their properties protect against oxidative stress and neuronal toxicity.

We went on to further test the role this five-compound combination plays in halting neuronal damage. We altered the concentrations of each compound within the mixture to test for an increase in effectiveness as compared to mixture with equal concentrations of each compound. We saw that when we increased the concentration of L, N, T, Pi and Py, respectively, most failed to work more effectively than the mixture containing equal concentrations of each compound. Surprisingly, we found that when we increased amount Pi six times more than the L, N, T and Py it worked very similarly, just slightly more effectively than the combination that contained equal amounts of the each compound (see Figure 12). Pi must have enhanced the mixture's potency when we altered the concentration because Pi is known to activate SKN-1/Nrf2 using the TRPA-1 receptor and signals through DJ1 and GLO1 to reduce methylglyoxal levels and neuronal damage (6). Therefore, when we increased the concentration of Pi results indicate that the

combination improved the mixtures detoxification capability. This finding suggests that Pi is critical for broadening the overall effectiveness of the combination. This combination is possibly enhancing the metabolism of α-dicarbonyls by increasing the amount of glutathione levels to reduce methylglyoxal stress.

These findings confirmed that our five-compound combination exerted neuroprotective effects and reversed methylglyoxal-induced damage by rescuing neurite retraction. We know that some compounds target the TRPA-1 receptor, while others independently target the Nrf2 transcription factor that is responsible for upregulating the glyoxalase system. Although these compounds in combination may target different parts of the TRPA-1 signaling pathway, together they ameliorate methylglyoxal toxicity by regulating methylglyoxal detoxification through the activation of the glyoxalases.

If we had more compounds to work with, for example, if we made a mixture that included ten different compounds rather than the five, I believe we would not see any further activation of the detoxification pathway. If we were to add more compounds to the mixture, I believe the mixtures would start to have similar effects or diminish their combined activity. Furthermore, the addition of more compounds to the mixture increases the chances of toxicity because each compound is solubilized differently. With more compounds, we run the risk that the compounds might not work well due to non-polar, polar properties, interference between agents, and/or chemical incompatibilities. Also, each compound is absorbed, metabolized, and excreted differently, which might become an issue if mixed together, resulting in the combination being unfavorable to our studies.

Test the best combination in various cell lines to confirm its therapeutic efficacy.

The two five- compound combinations were first identified using N27 cells; we saw that the two sets of five-compound mixtures had a significant capacity for ameliorating methylglyoxal stress. We then tested this phenomenon to confirm its therapeutic efficacy in two different cells lines: PC12 and SH-SY5Y. We see that in the cells treated with methylglyoxal, the neurites retract about to about 50 percent of the length compared to the untreated control. We saw that in both cells lines, the combinations overcame the damaging effects of methylglyoxal while the compounds used in isolation failed to reach full rescue. We see that the combinations did not have any toxic effects across all three mammalian cell lines, indicating their detoxification abilities are robust and broadly applicable. These compounds have been shown to exhibit antioxidant and neuroprotective effects in previous *in vivo* and *in vitro* studies (28,39,41)This unique combination was generated to increase the activity of the glyoxalase system, therefore enhancing the detoxification of methylglyoxal to mitigate α-dicarbonyl toxicity. These studies revealed two five-compound mixtures that had robust beneficial effects. The observation establishes combinatorial therapy as the better therapeutic approach.

Since we know that under physiological conditions, methylglyoxal is detoxified into a less reactive metabolite, D-lactate, we expect the administration of the combinations in the presence of methylglyoxal would result in an increased production of D-lactate. Therefore, to show that these combinations enhance the detoxification mechanism, a future experiment would be to measure elevated levels of D-lactate. Additionally, we would need to identify the combinations mechanism of action, to ensure

that the mixture is detoxifying methylglyoxal. A future experiment would be to perform RT-PCR to show if the combinations are targeting parts of the TRPA-1-Nrf2 signaling pathway.

Test the best combination in various cell lines to investigate its neuroprotective capacity against MPP^+-induced cellular damage.

We tested our combinations under MPP^+ stress in multiple cell lines to recapitulate the neurodegenerative effect in Parkinson's disease. We saw that in our negative control MPP^+ significantly reduced the neurite length of the cells, and the combinations rescued MPP^+-induced neuronal damage. We also compared how effective the single compounds were in mitigating MPP^+ damage. Results show that although, the single compounds ultimately alleviated MPP^+-induced neuronal stress, they never reach full rescue of the neurite length as compared to the control. However, the five-compound combination had a stronger therapeutic effect than both of compounds used insolation. The combined activity exceeds the total activity of the individual compounds indicating that our combination is largely synergistic. These results demonstrate that our combination exhibits neuroprotective activity against neurodegeneration in Parkinson's disease through rescue of MPP^+- induced neuronal damage. We believe to have found the best combination that not only mitigates neuronal damage under MGO stress but also exerts neuroprotective activity against MPP^+ stress. These findings show that our combination is unique, meaning that it is a mixture that contains a variety of beneficial, therapeutic properties working together to protect against the downstream effects of MPP^+, such as apoptosis, oxidative stress, and mitochondrial dysfunction. All, which are principal mechanisms, found to be associated with the early onset of both PD and

diabetes. And as stated in literature, drugs that are found to alleviate diabetic symptoms can also be beneficial for PD (39).

Validation in several mammalian in vitro studies permits further research in diabetic mouse model

Dose-dependent studies and validation of therapeutic efficacy toward MGO and MPP+ toxicity permits rationale for combinational supplementation in mammalian mouse model. Mice are often used to model diabetes and AGEs-related pathologies due to their relatively close link to human disease biology. In previous studies, individual compounds have been used as therapeutic supplements to exhibit anti-inflammatory, neuroprotective, and antioxidant effects. Many studies have used these compounds as a single supplement to decrease blood glucose levels, and also prevent diabetic complications such as cardiomyopathy, and neuropathy as well as nephropathy (29,41,57). However, there is a significant need to develop a therapeutic that ameliorates AGE-stress, so we have identified a five-compound mixture as a complementary treatment option for diabetic pathologies and neurodegenerative disorders, such as Parkinson's disease. Our combination includes many beneficial properties, which can be used as a potential therapeutic agent to improve glycemic levels and prevent formation of AGEs, thus prohibit secondary pathologies.

We postulate that the anti-inflammatory and antioxidant properties of the working compounds could play a role in their neuroprotective effect. We hope to translate this to *in vivo* studies; combinational and monotherapy has worked before in both clinical and *in vivo* studies (41,64). We believe our combination when used in a diabetic mouse model; the combination can potentially prevent diabetic complications by clearing out precursors

of AGEs and ultimately inhibiting the formation of AGEs. All these compounds are 'supplement-grade' meaning they are safe for human consumption. This allows for the ease of adapting the methods as all are already available.

Diabetic complications and age-associated neurodegenerative disorders such as Parkinson's diseases currently do not have effective drugs treatments. Current therapeutics available for diabetic patients target glucose levels to reach glycemic control. However, targeting blood glucose may not prevent the formation of AGEs. Hence, our unique supplement mix protects against neuronal damage *in vitro,* targeting the formation of AGEs by mitigating α-dicarbonyl toxicity. Together with current therapeutic is a complementary way to prevent the progression of diabetes and treat diabetic complications **(Figure 16).**

Our combination has the potential to serve as a powerful tool for treatment. However, in order to effectively translate our findings and achieve a desirable outcome, we need to first assess our results acquired *in vitro*. We have to take into account that ratios used to generate our combination may change dramatically once administrated to mice due differences in metabolism, absorption, distribution, and excretion. We will carefully choose a concentration and we are hopeful that our mixture will translate well to mice and ultimately humans.

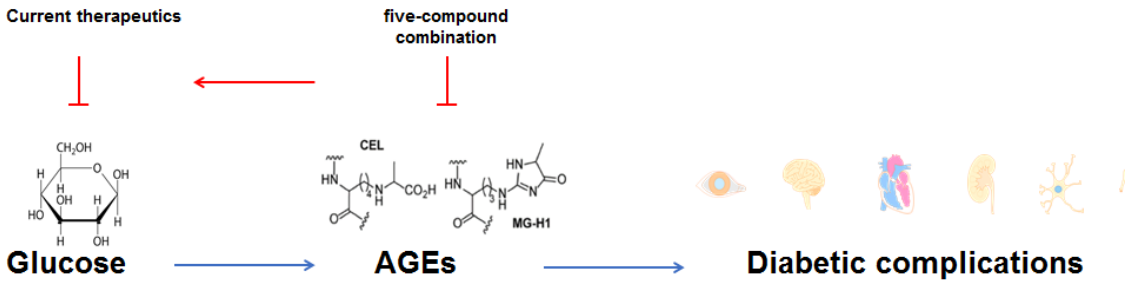

Figure 16: **Five-compound combinations as a possible therapeutic for diabetic complications.**
This illustration represents the critical factors that contribute to diabetic complications. High glucose levels lead to the formation of AGEs which accumulate in various tissues resulting in diabetes-associated pathologies. Current therapeutic target blood glucose levels and the five-compound combination target the formation of AGEs. Both, current therapeutic and the five-compound combination can be used as a supplement to treat diabetic complications.

Worm, mouse, and cell culture models suggest that AGEs influence diabetic complications and neurodegeneration, yielding future studies to understand the mechanism involved in modulating AGEs. Our combinations ability to detoxify precursors of AGEs suggests that we may have developed a therapeutic that alleviates AGEs-associated pathologies. We are moving towards mouse experiments soon and we are very hopeful that the mixture will show positive data *in vivo*. We will be using C57BKS *db/db* and high fat induced diabetes mouse models that exhibit diabetic-related complications. We plan to perform various non-invasive assays and histological studies to study amelioration of diabetic complications such as diabetic cardiomyopathy, diabetic nephropathy and diabetic neuropathy. We believe these compounds will modulate cellular stress due to α-dicarbonyls and advanced glycation end products, in turn, ameliorating diabetic compilations without manipulating glucose.

References

1. Alberti KGMM, Zimmet PZ. Definition, diagnosis and classification of diabetes mellitus and its complications. Part 1: diagnosis and classification of diabetes mellitus provisional report of a WHO consultation. Diabet Med. 1998;15(7):539–53.
2. Moraru A, Wiederstein J, Pfaff D, Fleming T, Miller AK, Nawroth P, et al. Elevated Levels of the Reactive Metabolite Methylgl1. Moraru A, Wiederstein J, Pfaff D, Fleming T, Miller AK, Nawroth P, et al. Elevated Levels of the Reactive Metabolite Methylglyoxal Recapitulate Progression of Type 2 Diabetes. Cell Metabolism. 2018; yo. Cell Metabolism. 2018;
3. Danaei G, Finucane MM, Lu Y, Singh GM, Cowan MJ, Paciorek CJ, et al. National, regional, and global trends in fasting plasma glucose and diabetes prevalence since 1980: Systematic analysis of health examination surveys and epidemiological studies with 370 country-years and 2·7 million participants. Lancet. 2011;378(9785):31–40.
4. Ninomiya T. Diabetes Mellitus and Dementia. Curr Diab Rep [Internet]. 2014;14(5):487. Available from: https://doi.org/10.1007/s11892-014-0487-z
5. Association AD. Diagnosis and classification of diabetes mellitus. Diabetes Care [Internet]. 2013;36 Suppl 1:S67-74. Available from: http://care.diabetesjournals.org/content/36/Supplement_1/S67.full%5Cnhttp://care.diabetesjournals.org/content/36/Supplement_1/S67.full.pdf%5Cnhttp://www.pubmedcentral.nih.gov/articlerender.fcgi?artid=2797383&tool=pmcentrez&rendertype=abstract%5Cnhttp://ww
6. Chaudhuri J, Bose N, Gong J, Hall D, Rifkind A, Bhaumik D, et al. A Caenorhabditis elegans Model Elucidates a Conserved Role for TRPA1-Nrf Signaling in Reactive α-Dicarbonyl Detoxification. Curr Biol. 2016;26(22):3014–25.
7. Han Y, Randell E, Vasdev S, Gill V, Gadag V, Newhook LA, et al. Plasma methylglyoxal and glyoxal are elevated and related to early membrane alteration in young, complication-free patients with Type 1 diabetes. Mol Cell Biochem. 2007;305(1–2):123–31.
8. Lange JN, Wood KD, Knight J, Assimos DG, Holmes RP. Glyoxal formation and its role in endogenous oxalate synthesis. Advances in Urology. 2012.
9. Thornalley PJ. Pharmacology of methylglyoxal: Formation, modification of proteins and nucleic acids, and enzymatic detoxification - A role in pathogenesis and antiproliferative chemotherapy. Vol. 27, General Pharmacology. 1996. p. 565–73.
10. Baig MH, Jan AT, Rabbani G, Ahmad K, Ashraf JM, Kim T, et al. Methylglyoxal and Advanced Glycation End products: Insight of the regulatory machinery affecting the myogenic program and of its modulation by natural compounds. Sci Rep. 2017;7(1).
11. Thornalley PJ. Protein and nucleotide damage by glyoxal and methylglyoxal in physiological systems--role in ageing and disease. Drug Metabol Drug Interact [Internet]. 2008;23(1–2):125–50. Available from: http://www.ncbi.nlm.nih.gov/pubmed/18533367%5Cnhttp://www.pubmedcentral.nih.gov/articlerender.fcgi?artid=PMC2649415

12. BERLANGA J, CIBRIAN D, GUILLÉN I, FREYRE F, ALBA JS, LOPEZ-SAURA P, et al. Methylglyoxal administration induces diabetes-like microvascular changes and perturbs the healing process of cutaneous wounds. Clin Sci [Internet]. 2005;109(1):83–95. Available from: http://clinsci.org/lookup/doi/10.1042/CS20050026
13. Golej J, Hoeger H, Radner W, Unfried G, Lubec G. Oral administration of methylglyoxal leads to kidney collagen accumulation in the mouse. Life Sci. 1998;63(9):801–7.
14. Riboulet-Chavey A, Pierron A, Durand I, Murdaca J, Giudicelli J, Van Obberghen E. Methylglyoxal impairs the insulin signaling pathways independently of the formation of intracellular reactive oxygen species. Diabetes. 2006;55(5):1289–99.
15. Kong X, Ma MZ, Huang K, Qin L, Zhang HM, Yang Z, et al. Increased plasma levels of the methylglyoxal in patients with newly diagnosed type 2 diabetes 2. J Diabetes [Internet]. 2014;6(6):535–40. Available from: http://www.ncbi.nlm.nih.gov/pubmed/24720446
16. Ceriello A, Motz E. Is Oxidative Stress the Pathogenic Mechanism Underlying Insulin Resistance, Diabetes, and Cardiovascular Disease? The Common Soil Hypothesis Revisited. Vol. 24, Arteriosclerosis, Thrombosis, and Vascular Biology. 2004. p. 816–23.
17. Uribarri J, del Castillo MD, de la Maza MP, Filip R, Gugliucci A, Luevano-Contreras C, et al. Dietary advanced glycation end products and their role in health and disease. Adv Nutr [Internet]. 2015;6(4):461–73. Available from: http://www.ncbi.nlm.nih.gov/pubmed/26178030%5Cnhttp://www.pubmedcentral.nih.gov/articlerender.fcgi?artid=PMC4496742
18. Brownlee, M.D M. ADVANCED PROTEIN GLYCOSYLATION IN DIABETES AND AGING. Annu Rev Med [Internet]. 1995;46(1):223–34. Available from: http://www.annualreviews.org/doi/10.1146/annurev.med.46.1.223
19. LV X, LV G-H, DAI G-Y, SUN H-M, XU H-Q. Food-advanced glycation end products aggravate the diabetic vascular complications via modulating the AGEs/RAGE pathway. Chin J Nat Med [Internet]. 2016;14(11):844–55. Available from: http://www.sciencedirect.com/science/article/pii/S1875536416301017
20. Heier M, Margeirsdottir HD, Torjesen PA, Seljeflot I, Stensæth KH, Gaarder M, et al. The advanced glycation end product methylglyoxal-derived hydroimidazolone-1 and early signs of atherosclerosis in childhood diabetes. Diabetes Vasc Dis Res. 2015;12(2):139–45.
21. Monnier VM, Sell DR, Genuth S. Glycation products as markers and predictors of the progression of diabetic complications. In: Annals of the New York Academy of Sciences. 2005. p. 567–81.
22. Xue J, Ray R, Singer D, Böhme D, Burz DS, Rai V, et al. The receptor for advanced glycation end products (RAGE) specifically recognizes methylglyoxal-derived AGEs. Biochemistry. 2014;53(20):3327–35.
23. Hofmann MA, Drury S, Fu C, Qu W, Taguchi A, Lu Y, et al. RAGE mediates a novel proinflammatory axis: A central cell surface receptor for S100/calgranulin polypeptides. Cell. 1999;97(7):889–901.
24. Juranek J, Ray R, Banach M, Rai V. Receptor for advanced glycation end-products in neurodegenerative diseases. Vol. 26, Reviews in the Neurosciences. 2015. p.

691–8.
25. Ravichandran R, Fang YS, Marie SA. Receptor for AGE (RAGE): signaling mechanisms in the pathogenesis of diabetes and its complications. Ann N Y Acad Sci [Internet]. 2011 Dec 23;1243(1):88–102. Available from: https://doi.org/10.1111/j.1749-6632.2011.06320.x
26. Agathos E, Tentolouris A, Eleftheriadou I, Katsaouni P, Nemtzas I, Petrou A, et al. Effect of α-lipoic acid on symptoms and quality of life in patients with painful diabetic neuropathy. J Int Med Res [Internet]. 2018 Mar 8;300060518756540. Available from: https://doi.org/10.1177/0300060518756540
27. Vallianou N, Evangelopoulos A, Koutalas P. Alpha-lipoic Acid and diabetic neuropathy. Rev Diabet Stud [Internet]. 2009;6(4):230–6. Available from: http://www.ncbi.nlm.nih.gov/pubmed/20043035%5Cnhttp://www.pubmedcentral.nih.gov/articlerender.fcgi?artid=PMC2836194
28. Daousi C, MacFarlane I a, Woodward a, Nurmikko TJ, Bundred PE, Benbow SJ. Chronic painful peripheral neuropathy in an urban community: a controlled comparison of people with and without diabetes. Diabet Med [Internet]. 2004;21(9):976–82. Available from: http://www.ncbi.nlm.nih.gov/pubmed/15317601
29. Packer L, Witt EH, Tritschler HJ. Alpha-lipoic acid as a biological antioxidant. Vol. 19, Free Radical Biology and Medicine. 1995. p. 227–50.
30. Packer L, Kraemer K, Rimbach G. Molecular aspects of lipoic acid in the prevention of diabetes complications. Nutrition [Internet]. 2001;17(10):888–95. Available from: http://www.ncbi.nlm.nih.gov/pubmed/11684397
31. Singh R, Kishore L, Kaur N. Diabetic peripheral neuropathy: Current perspective and future directions. Vol. 80, Pharmacological Research. 2014. p. 21–35.
32. Münch G, Lüth HJ, Wong a, Arendt T, Hirsch E, Ravid R, et al. Crosslinking of alpha-synuclein by advanced glycation endproducts--an early pathophysiological step in Lewy body formation? J Chem Neuroanat. 2000;20(3–4):253–7.
33. Dy SM, Bennett WL, Sharma R, Zhang A, Waldfogel JM, Nesbit SA YH, Chelladurai Y, Feldman D, Wilson LM RK. Preventing Complications and Treating Symptoms of Diabetic Peripheral Neuropathy [Internet]. Comparative Effectiveness Review. 2017. 1-233 p. Available from: https://www.ncbi.nlm.nih.gov/pubmedhealth/PMH0096158/pdf/PubMedHealth_PMH0096158.pdf
34. Santiago JA, Potashkin JA. System-based approaches to decode the molecular links in Parkinson's disease and diabetes. Vol. 72, Neurobiology of Disease. 2014. p. 84–91.
35. Wiemerslage L, Schultz BJ, Ganguly A, Lee D. Selective degeneration of dopaminergic neurons by MPP+and its rescue by D2 autoreceptors in Drosophila primary culture. J Neurochem. 2013;126(4):529–40.
36. Ariga H, Takahashi-Niki K, Kato I, Maita H, Niki T, Iguchi-Ariga SMM. Neuroprotective function of dj-1 in Parkinson's disease. Oxidative Medicine and Cellular Longevity. 2013.
37. Cereda E, Barichella M, Pedrolli C, Klersy C, Cassani E, Caccialanza R, et al. Diabetes and risk of Parkinson's disease: A systematic review and meta-analysis. Vol. 34, Diabetes Care. 2011. p. 2614–23.

38. Guerrero E, Vasudevaraju P, Hegde ML, Britton GB, Rao KS. Recent Advances in alpha-Synuclein Functions, Advanced Glycation, and Toxicity: Implications for Parkinson's Disease. Mol Neurobiol. 2012;47:525–36.
39. Aviles-Olmos I, Dickson J, Kefalopoulou Z, Djamshidian A, Ell P, Soderlund T, et al. Exenatide and the treatment of patients with Parkinson's disease. J Clin Invest [Internet]. 2013;123(6):2730–6. Available from: http://www.pubmedcentral.nih.gov/articlerender.fcgi?artid=3668846&tool=pmcentrez&rendertype=abstract
40. Sian J, Youdim M, Riederer P, Gerlach M. Biochemical Anatomy of the Basal Ganglia and Associated Neural Systems. In: Basic neurochemistry : molecular, cellular, and medical aspects. 1999. p. 26.
41. Singh S, Jamwal S, Kumar P. Neuroprotective potential of Quercetin in combination with piperine against 1-methyl-4-phenyl-1,2,3,6-tetrahydropyridine-induced neurotoxicity. Neural Regen Res. 2017;12(7):1137–44.
42. Murakami K, Kondo T, Ohtsuka Y, Fujiwara Y, Shimada M, Kawakami Y. Impairment of glutathione metabolism in erythrocytes from patients with diabetes mellitus. Metabolism [Internet]. 1989;38(8):753–8. Available from: http://www.ncbi.nlm.nih.gov/entrez/query.fcgi?cmd=Retrieve&db=PubMed&dopt=Citation&list_uids=2569661
43. Bierhaus A, Fleming T, Stoyanov S, Leffler A, Babes A, Neacsu C, et al. Methylglyoxal modification of Na v 1.8 facilitates nociceptive neuron firing and causes hyperalgesia in diabetic neuropathy. Nat Med. 2012;18(6):926–33.
44. Giacco F, Du X, D'Agati VD, Milne R, Sui G, Geoffrion M, et al. Knockdown of glyoxalase 1 mimics diabetic nephropathy in nondiabetic mice. Diabetes. 2014;63(1):291–9.
45. Mäkinen V-P, Civelek M, Meng Q, Zhang B, Zhu J, Levian C, et al. Integrative Genomics Reveals Novel Molecular Pathways and Gene Networks for Coronary Artery Disease. PLoS Genet [Internet]. 2014;10(7):e1004502. Available from: http://dx.plos.org/10.1371/journal.pgen.1004502
46. Wilson AF, Elston RC, Tran LD, Siervogel RM. Use of the robust sib-pair method to screen for single-locus, multiple- locus, and pleiotropic effects: application to traits related to hypertension. Am J Hum Genet. 1991;48(5):862–72.
47. Lee JY, Song J, Kwon K, Jang S, Kim C, Baek K, et al. Human DJ-1 and its homologs are novel glyoxalases. Hum Mol Genet. 2012;21(14):3215–25.
48. Lavernia F, Adkins SE, Shubrook JH. Use of oral combination therapy for type 2 diabetes in primary care: Meeting individualized patient goals. Postgrad Med. 2015;127(8):808–17.
49. Goldman-Levine JD. Beyond metformin: Initiating combination therapy in patients with type 2 diabetes mellitus. Vol. 31, Pharmacotherapy. 2011.
50. Hollander P, Sugimoto D, Vlajnic A, Kilo C. Combination therapy with insulin glargine plus metformin but not insulin glargine plus sulfonylurea provides similar glycemic control to triple oral combination therapy in patients with type 2 diabetes uncontrolled with dual oral agent therapy. J Diabetes Complications. 2015;29(8):1266–71.
51. Samra YA, Said HS, Elsherbiny NM, Liou GI, El-Shishtawy MM, Eissa LA. Cepharanthine and Piperine ameliorate diabetic nephropathy in rats: role of NF-κB

and NLRP3 inflammasome. Life Sci. 2016;157:187–99.
52. Xue M, Weickert MO, Qureshi S, Kandala N-B, Anwar A, Waldron M, et al. Improved Glycemic Control and Vascular Function in Overweight and Obese Subjects by Glyoxalase 1 Inducer Formulation. Diabetes [Internet]. 2016;65(8):2282–94. Available from: http://diabetes.diabetesjournals.org/lookup/doi/10.2337/db16-0153
53. Brings S, Fleming T, Freichel M, Muckenthaler MU, Herzig S, Nawroth PP. Dicarbonyls and advanced glycation end-products in the development of diabetic complications and targets for intervention. Vol. 18, International Journal of Molecular Sciences. 2017.
54. Beisswenger P, Ruggiero-Lopez D. Metformin inhibition of glycation processes. Diabetes Metab [Internet]. 2003;29(4):6S95-6S103. Available from: http://linkinghub.elsevier.com/retrieve/pii/S1262363603727931
55. Rodrigues T, Matafome P, Santos-Silva D, Sena C, Seiça R. Reduction of methylglyoxal-induced glycation by pyridoxamine improves adipose tissue microvascular lesions. J Diabetes Res. 2013;2013.
56. Metz TO, Alderson NL, Thorpe SR, Baynes JW. Pyridoxamine, an inhibitor of advanced glycation and lipoxidation reactions: A novel therapy for treatment of diabetic complications. Vol. 419, Archives of Biochemistry and Biophysics. 2003. p. 41–9.
57. Depeint F, Bruce WR, Shangari N, Mehta R, O'Brien PJ. Mitochondrial function and toxicity: Role of B vitamins on the one-carbon transfer pathways. Chem Biol Interact. 2006;163(1–2):113–32.
58. Onorato JM, Jenkins AJ, Thorpe SR, Baynes JW. Pyridoxamine, an inhibitor of advanced glycation reactions, inhibits advanced lipoxidation reactions: Mechanism of action of pyridoxamine. J Biol Chem. 2000;275(28):21177–84.
59. Tanaka Y, Uchino H, Shimizu T, Yoshii H, Niwa M, Ohmura C, et al. Effect of metformin on advanced glycation endproduct formation and peripheral nerve function in streptozotocin-induced diabetic rats. Eur J Pharmacol [Internet]. 1999;376(1–2):17–22. Available from: http://www.ncbi.nlm.nih.gov/pubmed/10440084
60. Zheng F, Zeng YJ, Plati AR, Elliot SJ, Berho M, Potier M, et al. Combined AGE inhibition and ACEi decreases the progression of established diabetic nephropathy in B6 db/db mice. Kidney Int. 2006;70(3):507–14.
61. Heusinkveld HJ, Westerink RHS. Comparison of different in vitro cell models for the assessment of pesticide-induced dopaminergic neurotoxicity. Toxicol Vitr. 2017;45:81–8.
62. Grau CM, Greene LA. Use of PC12 cells and rat superior cervical ganglion sympathetic neurons as models for neuroprotective assays relevant to parkinson's disease. Methods Mol Biol. 2012;846:201–11.
63. Jung GS, Lee KM, Park JK, Choi SK, Jeon WB. Morphogenetic and neuronal characterization of human neuroblastoma multicellular spheroids cultured under undifferentiated and all-trans-retinoic acid-differentiated conditions. BMB Rep. 2013;46(5):276–81.
64. Rabbani N, Xue M, Thornalley PJ. Dicarbonyls and glyoxalase in disease mechanisms and clinical therapeutics. Glycoconj J. 2016;33(4):513–25.